NASA

Technical Memorandum 79574

The Cosmic X-Ray Experiment Aboard HEAO-1

R. Rothschild, E. Boldt,
S. Holt, P. Serlemitsos,
G. Garmire, P. Agrawal,
G. Riegler, S. Bowyer,
and M. Lampton

June 1978

National Aeronautics and
Space Administration

Goddard Space Flight Center
Greenbelt, Maryland 20771

The Cosmic X-Ray Experiment Aboard HEAO-1

R. Rothschild*, E. Boldt, S. Holt, P. Serlemitsos,
Goddard Space Flight Center
Greenbelt, Md. 20771

G. Garmire, P. Agrawal†,
California Institute of Technology
Pasadena, Ca.

G. Riegler,
Jet Propulsion Laboratory
Pasadena, Ca.

S. Bowyer, and M. Lampton
Space Science Laboratory
University of California
Berkeley, Ca.

* Presently at University of California, San Diego
† Presently at Tata Institute of Fundamental Research, Bombay, India

ABSTRACT

The Cosmic X-Ray Experiment aboard the HEAO-1 observatory is described. The instrument consists of six gas proportional counters of three types nominally covering the energy ranges of 0.15-3 keV, 1.2-20 keV, and 2.5-60 keV. The two low energy detectors have about 400 cm^2 open area each while the four others have about 800 cm^2 each. A novel feature of this experiment is the dual field of view collimators that allow the unambiguous determination of instrument internal background and diffuse x-ray brightness. Instrument characteristics and early performance will be discussed.

I. INTRODUCTION

The HEAO Cosmic X-Ray Experiment (also known as the A-2 experiment) is designed to study the large scale structure of the Galaxy and the Universe at X-ray energies. Within the Galaxy, supernovae and stellar winds contribute to a million or so degree hot gas that fills a substantial fraction of the region between the stars. The presence of this hot gas is important for the dynamics of the cooler gas which is related to the rate of star formation. The A-2 experiment is providing a greatly improved map of the local distribution of this hot component. At higher X-ray energies, a non-thermal component of galactic emission should appear. Cosmic ray electrons, for example, are capable of producing a hard spectrum of X-rays, and mapping the hard X-ray emission will produce new information on galactic magnetic fields and the cosmic ray electron distribution.

On a vaster scale, aggregates of galaxies are filled with a more tenuous but much hotter gas. The study of this hot gas (plasma) may reveal new information about the early phases of galaxy formation, generation of the elements in stars, and cluster formation and evolution in the early history of the Universe.

Extragalactic compact sources, such as Seyfert Galaxies, bright radio galaxies, and quasi-stellar radio sources are being studied over a broad energy range of spectral emission. Most of these objects are the seat of strong nonthermal processes which are poorly understood

at present. The improved sensitivity and increased spectral coverage available to us from the HEAO A-2 experiment can provide new information on the physical setting and parameters of the energy sources, i.e., the spectral shapes and matter content along the line of sight to these objects.

When viewed over angular scales exceeding a few degrees the extragalactic X-ray sky is generally dominated by an isotropic flux of hard radiation, the origin(s) of which is a major puzzle being addressed by the A-2 experiment. A precision measurement of its spectrum will allow detailed comparisons with known extragalactic sources (e.g. clusters of galaxies). By a systematic survey of the entire sky, a small gradual deviation in isotropy such as would arise from our own (observers) velocity should be detectable, thereby defining the proper reference frame(s) for this extensive diffuse emission. A study of the small-scale fluctuations in the isotropy for this apparently "diffuse" flux will characterize the contributions of very distant discrete sources that are otherwise not readily resolvable, especially at higher energies.

X-ray astronomy has also provided us with some simple isolated systems in our own galaxy of the type physicists are looking for when investigating previously unexplored regimes of nature. For example, the behavior of matter and radiation in an astrophysical environment of extremely intense magnetic and gravitational fields may now be modeled quite precisely by measuring the X-ray pulsar emission of a compact rotating object in a binary stellar system; several such cases

are already known. We are now beginning to understand that the key observational requirement is for temporally coherent information over the complete X-ray spectrum from the softest X-rays characteristic of thermal emission through the hardest X-rays indicative of non-thermal processes. The A-2 experiment is particularly well suited for such studies in that the spectral band is remarkably complete for such sources, since the low energy absorption due to the intervening interstellar matter and the characteristic high energy cut-offs in emission are both typically well included. In the very soft X-ray band an order of magnitude improvement in sensitivity over previous surveys enables us to search for hot white dwarf stars, cataclysmic variables and old novae, which appear to be present at the lowest energies transmitted by the interstellar gas.

II. EXPERIMENT DESCRIPTION

One of the primary goals of the A-2 experiment is to study the diffuse component of the X-ray sky over a broad energy band. At energies above the 2 keV the sky is remarkably isotropic. In order to search for structure in this background radiation it is necessary to have the systematic effects associated with the local environment of the experiment reduced to a minimum and any residual effect must be understood to a high degree.

The Cosmic X-Ray Experiment consists of three types of multi-anode, multi-layer, collimated, gas proportional counters and their associated electronics. The detectors are designated HED (high energy detector) for

the xenon-filled counters covering the energy range 2.5-60 keV, MED (medium energy detector) for the argon-filled counter covering the band 1.2-20 keV, and LED (low energy detector) for the thin window, propane-filled, flow counters covering the range 0.15-3 keV. The configuration of the six detectors within the HEAO-1 observatory is shown in Figure 1. These choices allow a reasonable dynamic range to be covered without introducing nonlinearities into any of the elements. Many precautions have been taken to reduce extraneous background, and some novel features have been incorporated which permit the unambiguous extraction of the flux of sky X-rays from the total signal.

The multiwire detectors allow separate readout of alternating cells of the detectors (See Figs. 2 and 3). The mechanical collimator in front of each detector has been carefully designed to exploit this alternating feature in that the left cells (Fig. 3, L1,L2) are covered by one field of view and the right cells (Fig. 3, R1,R2) are covered by a field of view about a factor of two different, but coaligned. Since the right and left cells are identical and their signals pass through a common amplifier, the difference between the left and right cells is a direct measure of what is entering through the aperture.

An important consideration for the detector is the choice of field of view. The field of view should not be so small that the detector internal background dominates the incoming signal. On the other hand, too large a field of view forces the background studies to cover rather large solid angle elements of the sky and makes discrete source studies difficult in crowded regions of the galactic plane. Based on rocket

flight data using the detector design, a field of view of 3° x 3° would provide a diffuse flux signal greater than the internal background signal up to about 40 keV. In order to provide better source positions and higher resolution angular maps at the lower energies where the signal to background expected is very good, a 1 1/2° x 3° field of view (FOV) was included. On the offset detectors, a 6° x 3° FOV was incorporated to give a better signal to internal background spectrum during pointing. The field of view of a typical A-2 detector is shown in Fig. 4.

Since the intensity of the diffuse X-ray flux is proportional to the solid angle exposed, the detector counting rate due to the diffuse component viewed by the larger field of view section will be about twice that viewed by the smaller section. Since the internal background is independent of collimator field of view, the count rate due to the diffuse background and due to internal background can be determined simultaneously.

The one medium energy detector, one high energy detector, and the two low energy detectors do not have front layer anticoincidence, since these layers would be too strongly absorptive of the X-rays under study. Penetrating particles will be rejected by the fact that they pass through more than one layer of detection. Soft particle fluxes can be detected by the following consideration. The rate of events in the V2 layer of the detector adjacent to the counter side walls is only a function of penetrating radiation, since these cells do not view space through the collimator. The layers denoted M1, M2, and V1 all view through the collimator, and may be used to measure the soft

component that enters the detector. The low energy detectors have magnets in their collimators that raise the electron threshold energy for electrons entering the detector to about 40 keV as determined by laboratory measurements.

A final design feature included was more important for discrete source identification and study, but is also valuable for background measurements when sharp contrast is present. Four detectors (LED 1, HED 2, MED, and HED 3) are aligned to view along the +Y spacecraft axis, while the remaining two (LED 2 and HED 1) are offset 6° towards the +X spacecraft axis in the X-Y plane (see Figure 1). When a source transits the "deck" detectors it is followed six degrees later by a transit of the offset detectors. Transient bursts of electrons will appear at the same time in both detectors in general since they appear to cover a wide range of pitch angles to the Earth's magnetic field. Another important feature of the offset detectors is that when the "deck" detectors are pointed toward a faint source, the offset detectors provide a continuous measure of the background just six degrees away in the sky for background subtraction.

During normal scanning operations HEAO-1 rotates clockwise about the sunpointed +Z axis with a nominal 33 minute period. Hence, the four deck-mounted detectors view a given point on the sky about 30 seconds before the two offset ones. The spin axis is stepped 1/2° every 12 hours in order to remain pointed at the sun. Each observatory rotation provides a scan of a great circle 3° (FWHM) wide on the sky through the ecliptic poles.

The experiment associated electronics include the data director, analog and digital submultiplexer, interfact controller, command decoder, low voltage power supply, and gas control system. A complete set of detector electronics is mounted on each of the six independent detectors and consists of the front-end electronics (preamplifier plus post amplifier and shaping network, high voltage distributions, and test pulse generator input section), source encoder, data processing unit, test pulse generator, detector command decoder, detector programmer, low voltage converter, and high voltage converter. The Cosmic X-Ray Experiment is allotted 1200 bps of telemetry and 23 watts of 28 volt DC power.

DETECTORS

The proportional counters consist of a detector housing, a collimator, four layers of wire grids, a grid cover, a thin window, and the filling gas. Table 1 lists various parameters of the detectors. The detector housing, used in conjunction with the window-collimator assembly are relied upon to maintain a near constant gas pressure inside each detector, and to maintain, with a high degree of accuracy, the structural integrity of the sensitive gas volume under varying amounts of differential pressure across the window. The housing is fitted with a pumping/filling port for evacuation while outgassing all surfaces in contact with the counting gas and for filling the detector. The two-gas HEDs (HED 1 and HED 3) have a second port for evacuating and filling

the propane veto layer, and a second thin window that separates the propane veto layer from the main detector section. After assembly all detectors are heated to 80° C for one week while connected to a pumping system. This is to remove the trapped gases that might degrade detector performance with time. Figures 2a, b, c show cross sectional views of the three types of detectors employed. In order to reduce the X-ray flux entering the detector through the housing (primarily Compton X-rays from the diffuse X-ray flux), the HEDs and MED have shielding epoxied to the housing and sides of the collimator. In the case of the MED the shielding is 0.051 cm of copper and for the HEDs it is 0.152 cm of tin on top of 0.051 cm of copper. The LEDs are shielded only by the 0.234 cm of the aluminum housing itself.

The wire grids are aluminum frames 1.22 cm thick supporting arrays of 0.168 cm OD, 0.018 cm ID BeCu tubes which in turn support the stretched wire cathodes. Kel-F insulators, spaced every 1.22 cm on the frame support the anodes. Both the cathode and anode wires are made of 0.0051 cm stainless steel wire, silver plated and drawn to size. All wires are mounted while supporting a 50 gram mass. Spring loading of the wires allows them to survive both the vibration stress of launch and the distortions due to varying thermal environment. The only grid that is constructed differently is the top grid (nearest the collimator) of the two-gas HEDs, where vertical ground wire boundaries are replaced by stiff aluminum walls, that are used to support the inner window of those detectors, as well as to serve as ground planes.

The grid cover consists of copper laminated onto aluminum for the HEDs and aluminum only for the LEDs and MED. It is mounted on back of the last grid, serving as a ground plane for the last row of anodes. In addition, this cover shields the sensitive gas volume from the unused gas in the counter, the latter being a source of characteristic X-rays which would add to the detector's internal background. For the HEDs the grid cover also supports the Am^{241} calibration source assembly.

Within each detector cell-to-cell interconnections define seven outputs (see Figure 3) denoted L1, L2, R1, R2, V1, V2, and ALPHA. The LEDs and MED use the V2 output as both V2 and ALPHA since these detectors have no internal Am^{241} source. The sets of left and right anodes in data layer one and two form outputs L1, L2, R1, R2. These are appropriately combined in the test pulse generator input section of the front end electronics (see Figure 5a and b) to form outputs M1 and M2 which indicate which data layer triggered and carries the pulse height information. Two other sets of anodes V1 and V2 form an anticoincidence cup around the data layer set of anodes and are used to reject charged particles that penetrate the gas volume. For the two-gas HEDs V1 is comprised of the end cells of each grid of data layers 1 and 2 and the entire rear grid, while V2 is the propane veto layer. In the other detectors V1 includes all but the end cells of the rear grid, while V2 is formed from the end cells of all grids. The ALPHA output comes from the two anodes on either side of the Am^{241} source in the HEDs and is used to route calibration data.

COLLIMATORS

Directional sensitivity is accomplished by the use of a dual field of view collimator which provides the detector with two co-aligned sections having different width field of view in the scan direction. The two components of the collimator are configured to expose alternative sets of anodes (denoted left [L] and right [R] in the counter volume. Each scan across a point in the sky results in two independent exposures. This collimator design allows the unambiguous simultaneous measurement of both the diffuse X-ray flux and detector internal background. The systematic errors are drastically reduced since the measurements utilize the same gas volume, same analog electronics, the same pulse height analyzer, and the same high voltage supply on a given detector.

All collimator sections view 3° (FWHM) normal to the scan plane, and one of the dual field of view sections on each views 3° (FWHM) along the scan plane. The other section views either 1 1/2° or 6° along the scan plane, nominally. Table 2 gives the solid angles subtended by the various collimator sections on each detector.

The HED collimators are fabricated from hundreds of rectangular cross section copper tubes epoxied together to form a single unit that also supports the 0.0025 cm mylar window. The window is aluminized on both sides with 750 Å of aluminum in order to prevent static charge build-up on the window, to form a ground plane for the first grid layer, and to attenuate ultra violet flux entering the detector. HED 1 and 3

have a second 0.0025 cm aluminized mylar window to separate the propane veto layer from the xenon main volume. The MED collimator is similarly constructed from aluminum tubes, and supports the single piece 0.0076 cm Be window. Both MED and HED collimators are covered by 0.008 cm kapton heat shields, aluminized on the inboard side to improve the thermal balance.

The LED collimators are of a more complex design. Starting near the detector gas volume, the LED collimator consists of an egg-crate window support constructed from aluminum slats. A window support mesh is located between the window support and the 1 1/2 micron polypropylene window that is carbon coated to reduce ultraviolet transmission. This yields a total equivalent polypropylene window of 125 $\mu g/cm^2$ for a nominal LED window. The main collimator consists of a stack of BeCu etched-grid meshes with greater than 90% transmission. A plastic, egg-crate thermal precollimator above the main collimator acts as a thermal baffle which a) minimizes heat loss into space, b) minimizes temperature gradients within the detector gas volume, and c) avoids the X-ray transmission loss which accompanies thin film thermal shields. Each of the three parts of each collimator was partitioned into three panels in order to increase strength and improve the ease of assembly.

Because of heat loss all detector operational heaters are controlled individually and those on the LEDs are supplemented by heaters in the collimator structure to minimize temperature gradients. The LED collimator structures also house Cobalt Samarium permanent magnets

to act as magnetic brooms. They prevent low energy electrons from entering the gas volume which would raise the internal background. Testing of the flight units shows the magnetic brooms to be greater than 90% efficient in rejecting electrons below 40 keV.

The LEDs have movable acoustic covers which are closed during launch to protect the thin windows from severe acoustics and possible damage from small particles. Each cover is spring loaded for opening upon command and can be driven closed by a motor on command.

FRONT END ELECTRONICS

The front end electronics consists of the preamplifiers with their shaping networks, the high voltage distribution system and the test pulse generator input network. Figures 5a and b show the latter two sections combined. Each anode set is connected to the high voltage source through 250 MΩ to insure that the current drawn in the case of a direct short to ground is not high enough to reduce the voltage on other anode sections and to minimize damage if arcing occurs. The charge collected on an anode for a given event charges the .001 μf coupling capacitor which in turn is the input to the charge sensitive preamplifier.

The test pulse generator input section is a capacitive tee network that provides the input for test signals at the front of the charge sensitive preamplifier without significantly increasing the input capacitance seen by the amplifier. Thus the low level noise is determined by the capacitance of the detector itself. This section also contains

the pulse transformers used to merge the left and right anode section signals to form the M1 and M2 outputs. The amplifier section contains the charge sensitive preamplifier, filter network, and bi-polar amplifier. The voltage pulses are shaped to reduce microphonics and minimize dead time. The outputs of the nine amplifiers are then input to the source encoder for analysis.

SOURCE ENCODER

The source encoder is the heart of a detector's data analysis system. It serves three basic functions. The first is to apply the logic conditions dictated by its command state to the nine signal inputs to determine if an acceptable (i.e., X-ray) event has occurred; to determine which anode sections collected the charge; and to indicate whether or not it was a calibration event. Some of the logic criteria can be relaxed by command, but this is only used to analyze the performance of the detector and is not a normal data taking mode. The second function is to pulse height analyze acceptable events. Due to the limited telemetry available, a compression of the PHA address must occur. The initial 128 equal width pulse-height channels are compressed pseudo-logrithmically into 64 channels. The identification of the anode set that triggered (either L1, R1, L2 or R2 or M1, M2, V1 or V2 depending upon command) is included with the PHA channel number. The third function is to shape and output the data to the data processing unit (DPU) for subsequent analysis. The rate of acceptable events from various anode sets are sent to the discovery scalers, and the raw rates

of the discriminators are output to the housekeeping scalers in the DPU. A commandable combination of the acceptable events from the two main data layers (M1 and M2) are output as the Multiscaler rate for further analysis by the fast timing section of the DPU.

Each of the nine inputs from the detector feeds into its associated threshold detector pulser. All threshold detector pulsers (L1, M1, R1, L2, M2, R2, V1, V2 and Alpha) yield output logic pulses when the commanded thresholds are exceeded by the input signal. M1 may be set at one of three separate thresholds in addition to being turned off by command, while the other pulsers have two separate thresholds along with "OFF". The M1 analog signal is also tested for being above a set upper threshold. Such large signals veto acceptable events.

The M1, M2, V1 and V2 pulses are fed into the anticoincidence logic. An equal to or greater than 2, (≥ 2), output is obtained whenever any two or more of these input pulses occur simultaneously. Thus, in general, the occurrence of a ≥ 2 output indicates the event triggering the detector system is not an X-ray. This ≥ 2 pulse is used to inhibit subsequent processing of events.

The M1 event logic is used to select layer 1 events for pulse height analysis. Three modes are possible by command. Nominally an acceptable event is one for which only the left or right anode set triggers, only layer 1, and the event is not above the upper level threshold. The left-right-only requirement can be eliminated by command as can the only-layer-1 criterion. However, if the most stringent

requirements are relaxed by all, the interpretation of pulse height data will be less straightforward. The M2 event logic is independent of M1 event logic and similar to it.

The M1, M2, V1 and V2 and Alpha analog signals are fed through their associated delay lines (6.0 μs delay) into linear gates. The linear gates will not pass these signals unless opened (for approximately 5.5 μs) by the PHA event logic. The delay is provided to allow sufficient time for the PHA event logic to determine whether or not it is a bona fide event. The outputs of the five linear gates are fed into a pulse height to pulse width converter. The analog pulse passed by the opened linear gate charges a capacitor in this circuit to its peak voltage (proportional to the event energy). This capacitor is allowed to discharge linearly and a pulse is generated at its output during the discharge. Thus, the output pulse width during discharge is proportional to the event energy. This pulse is fed to an output gate. Also fed to the output gate is the 500 kHz crystal controlled square wave. After a minimum delay of 5.0 μs, to assure complete charging of the capacitor in the height to width converter, and at the next leading edge of an oscillator square wave an enable pulse is generated to start discharge of the capacitor and also start the output pulse train. Thus, the output pulse train will always start at the same place in the square wave and the capacitor discharge starts at the same time. This assures no jitter in the output train, thereby yielding an accurate digital reading. Hence, the signal

emerging from the output gate is a 500 kHz square wave pulse train, with the number of pulses proportional to the event energy.

The output pulses are counted and the output count is indicated by digital bits A, B, C, D, E, and F, where A is the LSB and F is the MSB. However, the counting is not linear, and yields a compressed output. The first 31 pulses are counted directly, pulses 32 to 63 are counted two at a time and pulses 64 to 127 are counted four at a time. It should be noted that, normally, for pulse trains with total pulses greater than 127, the output count will be limited to 63. However, when the readout mode is commanded such that it will not include the most significant bit (F), the output will be limited to 31. That is, pulse trains with total pulses greater than 31 will indicate 31.

Some time is required for conversion of the input signal peak amplitude into an output digial word during pulse hight analysis. This time is 2.0 μs per linear channel (500 kHz oscillator). Thus, this conversion time varies from 2.0 μs for Channel 1 to 2.0 x 127 = 254 μs for linear channel 127. This conversion time contributes to the pulse height analysis dead time, that is, the time during which a subsequent event cannot be pulse height analyzed. Provision is made for selection of a fixed or variable dead time by command. The fixed dead time is 322 μs, assuring conversion and readout to the DPU of the largest acceptable input signal. The variable dead time is the minimum delay possible and is equal to (2 x Linear Channel + 52) μs. The fixed 52 μs is due to the readout pulse, readout delay, reset delay and the reset pulse.

The range of pulse heights from the first data layer (M1) is divided into four preset contiguous windows. Provision is made for selection, by command, of events with energies falling into any combination of these windows. Similarly data layer two (M2) is divided into two windows. Table 3 shows the channel boundaries of these windows measured before launch and in terms of 128 linear channels covering the entire range. The energy range of these windows depends upon the gain of the detector. Only those windows selected by command will be present in the pulse height histograms and in the first four discovery scalers. Thus the proper normalization of the spectra is accomplished using these discovery scalers.

The discovery scalers are the event counters for the X-ray detectors. Discovery scalers 1-4 give the counts in layer one left and right, layer two left and right respectively that are pulse height analyzed. Discovery scalers 5-8 give the counts in various combinations of layers and windows as selected by command. Eight microsecond pulses drive the discovery scaler counters. The housekeeping rates go directly to the DPU for accumulation and readout. Any combination of the first four discovery scalers chosen by command forms the Multi-scaler rate. This rate is fed to the fast time section (Δt computer) in the DPU for temporal analysis. Finally the M1 discriminator rate is sent to the DPU's ratemeter. If this rate is ever greater than 10^6 in a major frame (40.96 s) the high voltage to that detector will be automatically shut off. This protects the counters from excessive

rates at all times. The detector must be commanded back on after such an event, since the high voltage does not automatically return.

DATA PROCESSING UNIT

This experiment contains six identical DPUs (one per detector) that receive the outputs of the source encoders in order to compute and format into buffer storage:

1) Pulses in eight 16 bit discovery scalers
2) Pulses in ten 24 bit housekeeping scalers
3) Events in one hundred twenty-eight 16 bit histogram channels
4) Fast Timing information about X-ray events (Δt computer)

The purpose of the DPU is to process the data from the source encoder under control of seven commands and spacecraft timing signals. It then formats this processed data into eight different output buffer shift registers (called port 0 through 7). The following is a description of each port and its function.

Port 0:

Direct Read Out of X-Ray Event PHA. This is an eight bit shift register that is read out serially. The eight bits were transferred from the source encoder in coincidence with a Histogram Read Out pulse, signifying a non-calibration event. This event is loaded into the shift register any time it is not being read out. Thus the data in the shift register is that of the latest event. No 6-bit to 5-bit compression occurs for this port.

Port 1:

Direct Read-Out of Calibration Events. This port is identical to port 0, with the exception that the pulse height data enters the shift register in coincidence with the Calibration Read-Out pulse.

Port 2:

Housekeeping Scalers Read Out. This is a 256 bit shift register that contains ten 24 bit words containing the housekeeping total count for the previous major frame, plus seven bits of DPU command status and nine zeros. The major frame pulse initiates transfer of data from accumulators to the shift register.

Port 3:

Δt Computer Read Out. The Δt computer receives a single input (Multiscaler Rate) from the source encoder. The Δt computer asks one of three questions (mode I, II, or III) depending upon command status:

I) Any event(s) in Δt: Δt = 1.25, 2.5, 5.0, or 10 ms?

II) How many events in Δt: Δt = 10, 20, 40, or 80 ms?

III) Time to the first eight events in Δt?

Δt = 80 ms, Resolution = 39.0625 μs or

Δt = 160 ms, Resolution = 78.125 μs.

The answers to the above questions are put into a 16, 24, or 64 bit shift register depending upon mode for read-out.

When in mode I the contents of a flip-flop are transferred to the appropriate bit of a 16 bit shift register at the beginning of a Δt interval. It is a "one" if one or more events were input to the DPU

on the Multiscaler line during the previous Δt interval. It is "zero" otherwise. The flip-flop is then reset to "zero", and is ready for the next Δt interval. In mode II the accumulator (which has been counting Multiscaler pulses during Δt) is locked and contents transferred to the output shift register at the end of the interval. The accumulator is also zeroed during this time. In mode III the Multiscaler pulse advances a three bit address counter. At each address a counter counts clock pulses until the next Multiscaler pulse changes the address counter. After 8 pulses are received in the Δt interval all counters are inhibited causing a dead time until the process repeats at the next interval. At the beginning of an interval the first address clock starts so that the next pulse received stops the first clock and starts the second. This continues until the time bin ends or the eighth pulse stops the eighth clock. Special cases are as follows:

a) clock pulses = 0 indicates that more than one event occurred within one clock pulse.

b) clock pulses = 253, 254, or 255 indicates that no pulses came in within 253-255 clock pulses or that one occurred in the last pulse.

Port 4:

8 LSB Read-Out of Discovery Scaler Rates. This port contains the eight least significant bits of the 16 bit discovery scalers. This information is transferred to the output buffer every 1.28 s.

Port 5:

8 MSB Bit Read-Out of Discovery Scaler Rates. This port contains the eight most significant bits of the 16 bit discovery scalers. These rates are transferred to the output buffer every 5.12 or 1.28 s, depending upon command.

Port 6:

Read-Out of 8-bit LSB of PHA Histogram Contents. This contains bits 1-8 of the contents of the 16-bit deep, 128 channel science PHA histogram. The accumulation time for port 6 is either 10.24 or 40.96 s as controlled by command. The dead time for the accumulations is 20 μs in the DPU, but is greater in the source encoder, which drives this input.

Port 7:

Read-Out of 8-bit MSB of PHA Histogram Contents. This contains bits 9-16 of the contents of the 16-bit deep, 128 channel science PHA histogram. The accumulation time is either 10.24 or 40.96 s as controlled by command. Dead times are the same for port 6.

Table 4 summarizes the function of the eight DPU ports along with the telemetry needed for a complete read-out of the data.

TEST PULSE GENERATOR

The purpose of the TPG is to provide a versatile tail pulse generator capable of performing amplitude sweep and coincidence testing of each detector. The TPG produced pulses (at 1.28 kHz) enter

the front-end of selected preamps via the TPG input section. Starting at the beginning of a major frame the pulse amplitude increases linearly with time from zero until $(2)^{15}$ pulses occur (25.6s). The maximum amplitude is such that the final preamp outputs are above channel 124 but below channel 126 (the upper level threshold is set at a voltage equivalent to greater than channel 128 to insure the counting of all $(2)^{15}$ TPG pulses). This maximum TPG ramp voltage is presented to the analog housekeeping and read to a precision of 1/256. Selection of preamps to be stimulated is controlled either by command (manual mode) or by a hard-wired 24 position program (automatic mode). The TPG is inoperative when power is first applied, and remains so until the ABORT command is set to zero and a start pulse is received. Once started in the automatic mode, the TPG runs through the entire program in 15.7 minutes and then aborts itself. The TPG may be stopped at any time with an ABORT or TPG power-off command. In the manual mode the TPG runs through the one commanded combination of preamps repeatedly, with each start synched to the major frame pulse, until either ABORT is sent or power is removed.

HIGH VOLTAGE

Each supply is manually programmed to operate at an expected nominal voltage which is a function of the detector (HED, MED, LED) Four bit binary coded commands select the actual operating voltage output. Each binary command will change the output voltage 33 V. The supply will operate at any selected voltage with a stability of $\pm$ 0.2%

over all line, load, and temperature variations for the top eight voltage steps. The stability is ± 0.4% over these conditions for the lower eight voltage steps.

In the event that the control loop opens, a second, passive loop prevents the output voltage from exceeding a voltage no greater than 600 V above the nominal setting. The telemetry readout provides a 0 to 5 volt output (proportional to the high voltage value) that applies over the upper eight and the lower eight settings independently. This provides a telemetry resolution of greater than 20 MV/V. The output ripple is less than 1 mV (peak-to-peak). Transient response to worst case step commands causes no overshoot greater than 4% and with a time duration of less than 100 ms.

There are two "high voltage on" commands for each detector. One is simply "high voltage on", no questions asked. The other is "high voltage on" if propane gas pressure is above some threshold value. The latter is the preferred command. If the propane pressure drops, the electronic edge generated by the pressure flag going from high to low digitally turns off the high voltage. If the preferred "high voltage on" command is then sent, nothing will happen since the flag is low. If the other command is sent the high voltage will come on and not be automatically turned off since the edge and not the level is responsible for turn off. The HEDs turn off at 4.2 psi and the LEDs at 1.8 psi. The HED pressure must rise above about 5 psi to reset the flag, whereas the LEDs re-arm at about 3 psi.

DATA DIRECTOR AND ALLIED EXPERIMENT ELECTRONICS

The Data Director is part of the Data Collection System which gathers, schedules, selects and commutates the data from the six detector DPUs and two housekeeping submultiplexers into a single output through the Interface Controller to the spacecraft telemetry transmission system. The Digital Sub-Multiplexer provides the timing whereby digital housekeeping data from eight data sources are transmitted to the Data Director. Data channels are selected in a preprogrammed sequence. The Analog Sub-Multiplexer contains an analog-to-digital converter to transform analog voltage samples into eight-bit digital words. Data are then read out through the Data Director. The Interface Controller comprises the junction between incoming timing and command signals to the systems and outgoing data transmission from the experiment. Separate from, but associated with, the Data System is the Command System(Experiment Command Decoder and Detector Command Decoder) for reception and execution of ground commands, and the Experiment Programmer (power control and distribution) and Converter system (28 Vdc spacecraft supply to various circuit voltages).

The Data Director generates the control and timing signals necessary to create the telemetry format for the Cosmic X-Ray Experiment. The format information is stored in three banks of memory located in the Data Director. Two of these memories are fixed-format Read Only Memories (ROM). The third is a variable-format Sequential Access Memory (RAM).

The telemetry word frame (20 milliseconds) contains 16 slots for spacecraft telemetry words, each word is eight bits. Three of these words are allocated to the Cosmic X-Ray Experiment. Every sequence, or 1.28 seconds (four minor frames), the experiment must transmit 192 words to the spacecraft telemetry system. A major frame takes 40.96 seconds and consists of 32 sequences.

The ROMs contain 384 words of format information with each word being accessed once every two sequences. The RAM contains 192 words with each word being accessed every sequence. The RAM is programmed by ground command, and can be dumped to check its contents through the Digital Sub-Multiplexer housekeeping words. The six Data Processing Units plus the Analog Sub-Multiplexer and the Digital Sub-Multiplexer are the eight channels of data to be selected. This user selection information is coded using three bits of memory.

Any of the three banks of memories (ROM I, ROM II, RAM) can be selected by a two-bit code from the Experiment Command Decoder. The selected memory becomes effective at the beginning of the next major frame after receipt of the memory select command.

The Digital Sub-Multiplexer commutates eight channels of digital housekeeping data, including the Data Director. During the normal mode of operation the Data Director transfers 12 digital housekeeping works to the Digital Sub-Multiplexer every major frame. Eight of these words are words from the current ROM or RAM in use. A major frame counter is used to determine which memory words are transmitted.

Since a total of 384 ROM words must be sent, it will take 48 major frames (32.768 minutes) to complete this operation. The RAM is read out in 24 major frames or 16.384 minutes.

Two other modes can co-exist within the Data Director. The RAM can be loaded with new format information sequentially through a serial command data line and the contents of the RAM can be dumped through the Digital Sub-Multiplexer housekeeping words. The RAM cannot be loaded or dumped while it is the operating memory. Likewise, the RAM cannot be the memory selected for normal operation while it is in the load or dump mode. The RAM cannot be loaded and dumped at the same time.

Since the dump command is asychronous, RAM readout will not begin until the next major frame after receipt of this command. However, data requests can occur before the next major frame pulse is received. As an indication that the dump command was detected, the Data Director will send back to the Digital Sub-Multiplexer only "ones" until the next major frame pulse occurs. It then takes three major frames, or 2.048 minutes, to complete the dump via the Digital Sub-Multiplexer.

CALIBRATION SOURCES

All A-2 detectors contain internal Fe^{55} radioactive sources that shine into the end cells (V2 and also V1 for the two gas HEDs). The counting rate in the veto layer is low so as not to affect the layer's ability to reject charged particles. Upon command, the data collection

mode can be changed to include pulse height analysis of the veto layers V1 and V2. The position of the line, and thus detector gain, can be measured. In the HEDs and the MED, this is the 5.96 keV Mn $K_{\alpha\beta}$ line and in the LEDs it is the 1.74 keV $K_{\alpha\beta}$ line of the silicon which is fluoresced by the Fe^{55} source. A further use of this source is to measure the X-ray absorption of the propane veto layer (V2) in the two gas HEDs. By comparing the rates in V1 and V2, changes in absorption can be noted (for instance, due to xenon leaking into the propane layer).

The LEDs and the MED also have a commandable, rotatable, calibration source, that is mounted in the collimator. This consists of a radioactive source inside a hollow rod with a hole opposite the source. This rod is mounted on the shaft of a pulsed motor enabling it to be rotated $\pm$ 90°. In the exposed position, the source radiates through the hole in the rod into the detector, while in the unexposed position it is rotated 90° so that the detector is shielded from the X-rays by the rod wall. Surrounding the source rod is another hollow tube (called the source shield) with a hole in one side. This is mounted on the shaft of another pulsed motor. In the event the source rod sticks in the exposed configuration, the shield can be rotated such that it blocks the X-rays entering the detector. Future calibrations can then be made by rotating the shield.

The radioactive source for the MED source rod is Fe^{55} which has a half life of 2.7 years. The LED rods contain Cm^{244}, and alpha

emitter with a 17.9 year half-life. The alphas are shielded from the detectors and fluoresce targets of carbon, teflon, and aluminum whose $K_{\alpha\beta}$ X-rays can enter the detector. There are higher energy X-rays associated with Cm^{244} and they necessitate a graded shield on both the source rod and source shield.

The HEDs contain an internal Am^{241} source that emits an alpha particle coincidently with Np X-rays. The source is situated between the two anodes designated ALPHA (see Figure 2c). When an alpha particle is detected by these anodes, any X-ray event happening simultaneously is tagged as a calibration event. This is a very weak source so that it does not affect the science data dead times or spectra.

GAS CONTROL SYSTEM

Since the propane diffuses through the thin LED windows, it must be replaced to maintain detector pressure. Also, since there is a chance that the propane layer of the two gas HEDs may become contaminated (e.g. with xenon), a method is needed to exhaust and refill this layer. This indicates the need for an active gas replenishment system for the propane. Figure 6 shows the gas system with valves, pressure transducers, and regulation systems.

Propane is stored as a liquid in the reservoir whose pressure is monitored by an absolute transducer. The propane then travels to the two redundant (only one "on" at a time) regulator arms where the liquid is incrementally fed to a heat exchanger coil which vaporizes the propane.

The incremental feed is achieved by a digital regulator which consists of a solenoid valve commanded open or closed by a pressure transducer at the valve outlet. A pneumatic pressure regulator then reduces the pressure of the propane gas emerging from the heat exchanger to 17 psi for distribution to the various detectors.

At the outlet of the heat exchanger is a pressure switch which in the event that the pressure exceeds 50 psi disables the prime digital regulator, closes the arm's latching solenoid valve and starts up the other arm of the system. This prevents large quantities of liquid propane from entering the heat exchanger (and eventually the pressure regulator) if the digital regulator solenoid valve should fail open. If the second arm then fails the entire system shuts down and does not reactivate until commanded to do so.

It is desirable that the LEDs maintain a constant density (and thereby, constant gain). This is achieved by sensing the differential pressure between the detector volume and the reference volume, which is filled to the desired propane density before launch. Each LED has its own gas control loop which opens the fill solenoid for underpressure and opens the exhaust solenoid for overpressure. The pressure bandwidth is 1% of nominal pressure. The detector absolute pressure is also monitored. In the case of a failure of a detector gas loop, the loop can be disabled, the LED interconnect latching solenoid valve can be opened and the remaining gas loop can control both detectors.

The LEDs can, also, be purged using this system. In the purge

mode both the fill and exhaust valves are opened and the regulation bandwidth is widened to 50% of normal pressure. Eight to twelve minutes after receipt of the purge command the exhaust valve closes and the system returns to the regulate mode with its narrow bandwidth.

Protection in the gas loops is provided by the purge fault and valve fault detection circuitry. Valve fault detection integrates separately the time the fill valve and the exhaust valve are open each major frame. If the fill is open greater than 16 seconds or the exhaust is open greater than 8 seconds in a major frame, that LED's gas loop is shut down. Purge fault detection is a parallel timing circuit associated with the purge cycle. Normally the purge ends about a minute before this circuit and returns the gas loop to the regulate mode. If the protect circuit times out first, that LED's gas loop is shut down.

The LEDs also have pop-off valves on the exhaust lines. This not only is in-flight over-pressure protection but also bleeds the detector pressure down during the ascent portion of launch. The pop-offs are set at 0.5 psi.

In the event of a contaminated HED propane layer the gas can be vented and then the layer refilled to ~7 psi. To vent the propane layer of a given two-gas HED, the passive gas control system is enabled and the appropriate exhaust valve opened. Once the layer is evacuated the exhaust valve is closed and the HED main latching solenoid valve is opened. Filling is accomplished by a series of commands to the fill

solenoid valve. For each command received the valve opens once for ∿700 ms. This corresponds to about 0.3 psi per pulse. By monitoring the propane layer pressure after each pulse, the proper pressure can be attained.

III. EXPERIMENT PERFORMANCE

HEAO-1 was launched at 6:29 UT on August 12, 1977, into a circular orbit with an apogee of 445 kilometers and an inclination of 22.75 degrees. The orbital period is 93 minutes, with a nominal observatory revolution period of 33 minutes. Within a week after launch all A-2 detectors were turned on and functioning nominally.

The LED detector background is very low relative to the flux of X-rays observed from the sky. As part of the LED turn-on procedure during the first week in orbit, several orbits of data were taken with the protective covers closed. These covers are mainly low atomic number plastic material plus a thin aluminum foil covering. Figure 7 shows the pulse height histogram for detected X-rays from a bright region of the sky in Hercules, a typical sky region, viewing the dark Earth, and with the protective covers closed. As can be seen in this figure, the cover closed data lies somewhat below the flux observed when viewing the dark Earth. Sunlit Earth is very bright below 1 keV due to fluorescence of atmospheric oxygen and nitrogen produced by the illumination of the earth by solar X-rays. The dark Earth flux may be due in part to scattering of the cosmic background X-rays and in part by precipitation of trapped electrons into the upper atmosphere with subsequent bremsstrahlung.

In order to evaluate the effectiveness of the LED anticoincidence system against charged particle events, the rate of Earth events was monitored as a function of the charged particle flux over different geomagnetic latitudes. Figure 8 shows the count rates for the large and small fields of view for LED 1 as a function of cosmic ray rate (anticoincidence rate). There is no noticeable trend in Earth flux versus charged particle rate.

Occasionally, while the LED detectors were scanning across the dark Earth, an increase in the X-ray counting rate was observed which peaked while the collimators were perpendicular to the local magnetic field vector. This effect is much more prominent when viewing the dark Earth, since the Earth flux is so low. Using the V2 rates discussed earlier, it was found that charged particles were in fact present at this time. Figure 9 shows a plot of the "X-ray" flux from the Earth as a function of the charged particle flux for the two different fields of view of the detector in the 1/4 keV channel (0.15 - 0.30 keV). The low energy charged particles seem to be present everywhere in the HEAO-1 orbit. The distribution of particle arrival directions is fairly sharply peaked perpendicular to the magnetic field as can be seen from the plot in Figure 10. This figure shows the rate of "electrons" in LED 1 as a function of angle between the magnetic field vector and the detector look angle. The contribution of these particles to the X-ray signal in the 1/4 keV channel is relatively small, but the possibility of spectral variations in this component

could change the slope of the correlation. This possibility is still under investigation.

One final effect was uncovered by noting the sky intensity as the detectors scanned toward the Earth's horizon. This was the appearance of a horizon brightening even when the spacecraft was on the opposite side of the Earth from the sun. The origin of this brightening is not understood, but is clearly seen in Figure 11. This figure displays the 1/4 keV counting rate as a function of the angle to the center of the Earth for the two fields of view on LED 1. The data was taken during a point at SS Cygni while the Earth slowly occulted the source as a result of HEAO-1's orbital motion. The possible contamination of sky data by this effect limits the useful viewing angles to those greater than 90^{o} from the center of the Earth.

The charged particle monitoring capability of the detectors using the side veto layers and the elimination of data which is too near the Earth's horizon make it possible to construct diffuse X-ray maps of the sky which should be free of systematic or locally produced effects down to a level of better than about 10% of the diffuse sky flux in the 1/4 keV channel. Near 1 keV, the middle layers of the LED detectors are very insensitive to contamination and we may hope to detect anisotropies down to a few percent of the 1 keV diffuse sky signal.

The in-orbit performance of a HED detector is exhibited in Figure 12, where the effectiveness of the dual collimation scheme is quite evident. These histograms are based on data accumulated over many scan cycles regardless of what was in the field of view, be it the Earth or

celestial sources. The telemetry frames selected were those for which there were not bit errors and where the flux of ambient electrons ($\gtrsim$ 100 keV) entering the collimator was less than ~ 5 $(cm^2 \text{ sec sr})^{-1}$

The histogram for each of the fields of view exhibits two clearly separated peaks, the high one attributed to exposures dominated by the sky and the one with lower counts attributed to exposures dominated by the Earth. If there were no extraneous sources of background the two histograms would scale as the ratio of solid angles (i.e., both the Earth and the sky represent essentially isotropic sources). In fact, the Earth is a relatively weak X-ray source, even in the hard X-ray band ($\sim$ 3-60 keV) considered here, and most of the signal when the Earth fills the field of view arises from background internal to the detector (e.g. Compton collisions of gamma rays). More extensive data bear out the qualitative indication in Figure 12 that the internal background to be associated with the two fields of view are equal. Furthermore, a comparison of the internal background derived from the two peaks associated with the diffuse sky has been shown to be the same as that derived from the two peaks associated with the diffuse Earth, both in magnitude and spectral shape. As shown in Figure 12 by a dashed line, the internal background for HED 1 represents an average contamination of $\sim$ 14% for the large field of view (3° x 6°) and a $\sim$ 25% for the small (3° x 3°) when the full energy bandwidth is included.

Figure 13 displays the accumulated counting rate in 1/2 bins versus satellite scan angle for 1977 August 21 using non-Earth occulted data

with minimal charged particle contamination. The data are from the 3° x 3° sections of the three types of detectors and show how the diffuse sky flux varies in broad energy ranges. The strongest source in the field of view was 4U0305 + 41 (Perseus Cluster) at scan angle of 158° which exhibits little, if any, 1/4 keV emission while being easily detected in the 8-70 keV band.

The complex of sources in the Large Magellanic Clouds contributes to the enhancement near 270° scan angle, while the galactic plane crossing is near 320°. The anisotropic 1/4 keV diffuse background signal is evident as a function of scan angle while at higher energies the anisotropies diminish significantly.

Figure 14 shows count rates referred to scan angle on the sky from the 3° x 3° section of HED 1. As demonstrated here for the data superposed from many scans, the internal background has the effect of a constant offset and that the signal from a relatively weak source such as AM Her is clearly well above any sort of noise. An Abell cluster (A2256) was at the edge of the field of view at scan angle $\sim$ 103° during this time.

The HED propane veto layer has proven to be remarkably effective in reducing electron contamination. As already indicated for the data in Figures 12 and 14, we restricted ourselves to samples of relatively low electron flux; this eliminated $\sim$ 30% of the data. At this level, we have determined that less than 3% of the internal detector background arises from electrons.

IV. ACKNOWLEDGEMENTS

The authors would like to thank the following people and groups for their hard work over the years in preparing the A-2 experiment: R. Browning (HEAO Project Manager at GSFC), F. McDonald (HEAO-1 Project Scientist), D. Wrublik (A-2 Experiment Manager at GSFC), R. Martin (Systems Engineer), C. Glasser and the GSFC X-Ray Group laboratory staff (Detector Systems), W. Sours (Mechanical Systems), J. Robinson (Gas Systems), J. Westrom (Power System), J. Webb (Thermal System), D. Studenick (Collimator Development), E. Grandholm at Bendix Aerospace (LED Collimator Development), C. Cancro (Detector Signal Processing Electronics), H. White (Data Processing Electronics), F. Link (Data Format Electronics), J. Libby (Electrical Control System), J. Vu at CIT (Special LED Related Systems), H. Primbsch at UCB (Test Pulse Generator Design), R. Porter (Electrical Integration), K. Rosette (Mechanical Integration), R. Morgan (Integration Management), F. Marshall, Ian Touhey, P. Charles (scientific support), J. Lindner (Assistant Project Manager for Experiment Integration at TRW), F. Speer (HEAO Project Manager at MSFC), and D. Talley (A-2 Experiment Manager at MSFC).

TABLE 1 DETECTOR PARAMETERS

	LED 1	LED 2	HED 1	HED 2	MED	HED 3
DETECTOR NUMBER	0	1	2	3	4	5
ENERGY RANGE (keV)	.15-3	.15-3	2-60	2-60	1.5-20	2-60
DETECTION GAS	PROPANE	PROPANE	XENON+	XENON+	ARGON+	XENON+
GAS PRESSURE (TORR)	200 (0°C)	200 (0°C)	760 (20°C)	760 (20°C)	760 (20°C)	760 (20°C)
COLLIMATION LEFT	1.55 x 2.95	4.15 x 2.80	2.91 x 2.81	2.91 x 2.81	2.94 x 2.90	2.91 x 2.81
(DEG. FWHM) RIGHT	2.80 x 2.55	2.70 x 2.75	5.92 x 2.81	5.92 x 2.81	1.40 x 2.90	1.44 x 2.81
OPEN AREA LEFT	176.5	228***	418.0	418.0	390.7	418.0
(CM^2) RIGHT	205.4	205***	425.9	425.9	363.0	402.4
TOTAL OPEN AREA (CM^2)	381.9	433***	843.9	843.9	820.4	820.4
POSITION	DECK	OFFSET	OFFSET	DECK	DECK	DECK
WINDOW MATERIAL	POLYPROPYLENE	POLYPROPYLENE	MYLAR*	MYLAR**	BERYLLIUM	MYLAR*
WINDOW THICKNESS (CM)	1.4×10^{-4}	1.4×10^{-4}	5.1×10^{-3}	5.1×10^{-3}	7.6×10^{-3}	5.1×10^{-3}
LAYER DEPTH (CM)						
M1	1.372	1.372	1.372	1.372	1.372	1.372
M2	2.438	2.438	1.219	1.219	2.438	1.219
V1	1.372	1.372	1.372	1.372	1.372	1.372
V2	-	-	1.219	-	-	1.219

\+ plus 85 torr methane (20°C)

* plus 1.219 cm veto layer containing 380 torr propane (20°C) and 445 torr Neon (20°C) and 1500 Å aluminizing.

** plus 1500 Å aluminizing.

*** preliminary

TABLE 2 COLLIMATOR SOLID ANGLES

DETECTOR	COLLIMATOR	SOLID ANGLE	
		deg^2	msr
LED	3x3	8.11	2.47
	3x1½	4.70	1.43
	3x6	13.44	4.10
HED	3x3	8.18	2.49
	3x1½	4.05	1.23
	3x6	16.64	5.07
MED	3x3	8.53	2.60
	3x1½	4.06	1.24

TABLE 3 DETECTOR WINDOW AND THRESHOLD SETTINGS

	LED 1		LED 2		HED 1		HED 2		MED		HED 3	
	CH	keV*	CH	keV*	CH	keV†	CH	keV†	CH	keV†	CH	keV†
M1 LOW	6.5	.152	6.4	.150	3.2	1.0	3.0	1.0	7.7	1.0	3.3	1.0
M1 MID	9.0	.211	9.0	.211	5.1	2.0	4.9	2.0	10.7	1.5	5.2	2.0
M1 HIGH	11.3	.265	11.8	.277	7.1	3.1	6.9	3.1	17.2	2.5	7.2	3.1
L1 HIGH	10.1	.237	9.9	.232	7.1	3.1	6.8	3.1	12.9	2.0	7.2	3.1
R1 HIGH	10.0	.234	10.3	.241	7.0	3.1	6.9	3.1	12.8	2.0	7.2	3.1
W1A/W1B	18.4	.431	18.0	.422	12.7	6.0	12.4	6.0	38.9	6.0	13.0	6.0
W1B/W1C	31.6	.741	30.7	.720	15.5	7.5	15.1	7.5	48.3	7.5	15.9	7.5
W1C/W1D	85.4	2.002	81.4	1.908	65.0	31.9	63.4	31.9	63.5	10.0	66.3	31.9
M2 LOW	6.7	.157	7.4	.173	3.2	1.0	3.2	1.0	7.5	1.0	3.3	1.0
M2 HIGH	12.5	.293	14.5	.340	5.0	2.0	5.0	2.0	12.7	2.0	5.2	2.0
L2 HIGH	11.2	.263	12.0	.281	7.1	3.1	7.1	3.1	12.5	2.0	7.2	3.1
R2 HIGH	11.1	.260	12.2	.286	7.0	3.1	7.1	3.1	12.5	2.0	7.3	3.1
W2A/W2B	34.4	.806	35.6	.834	68.0	31.9	65.2	31.9	24.7	3.9	67.3	31.9
V1 LOW	7.0	.164	8.8	.206	3.1	1.0	3.2	1.0	7.6	1.0	3.3	1.0
V1 HIGH	11.0	.258			5.2	2.0	5.3	2.0	14.0	2.0	5.3	2.0
V2 LOW	7.1	.166	5.8	.136	3.2	1.0	3.2	1.0	7.6	1.0	3.8	1.0
V2 HIGH	11.0	.258			5.3	2.0	5.4	2.0	14.1	2.0	7.7	2.0

† Assumes Nominal High Voltage Setting (i.e. Nominal Gain)
* Assumes 3,000 keV = 128 ch, No Offset

Table 4

DPU PORT TELEMETRY RATES PER DETECTOR SUMMARY

PORT	SAMPLE TIME			RATE (bps)
0	Depends upon sample period. Example:			
	2.56s			3.125
1	Depends upon sample period. Example:			
	2.56s			3.125
2	40.96s			6.250
3	Mode I	Δt = 1.25ms		800
		= 2.50ms		400
		= 5.00ms		200
		=10.00ms		100
	Mode II	Δt = 10ms	8 bit	800
			12 bit	1200
		= 20ms	8 bit	400
			12 bit	600
		= 40ms	8 bit	200
			12 bit	300
		= 80ms	8 bit	100
			12 bit	150
	Mode III	Δt = 80ms		800
		= 160ms		400
4	1.28s			50
5	1.28s			50
	5.12s			12.50
6	10.24s			100
	40.96s			25
7	10.24s			100
	40.96s			25

FIGURE CAPTIONS

Figure 1 Configuration of the six detectors within the Cosmic X-Ray (A-2) Experiment and its position in the HEAO-1 observatory. The three axes of the spacecraft are labeled and the sense of the rotation is shown.

Figure 2 a) Cross-sectional view of an LED.

b) Cross-sectional view of the MED and HED 2. HED 2 also has an AM^{241} calibration unit mounted on the rear of the last set of grids as is on the other HEDs.

c) Cross-sectional view of HED 1 and 3.

Figure 3 Detector grid connections. Cell-to-cell anode interconnections are labeled.

Figure 4 Schematic illustration of typical collimator fields of view. All collimators have 3° FWHM fields of view normal to scan path. Parallel to the scan path are 3° FWHM and either 1 1/2° or 6° FWHM fields of view. Hence θ = 1 1/2° or 3° FWHM, depending upon the detector (see Table 1 for the fields of view of given detectors).

Figure 5 a) High voltage distribution and test pulse generator input section for LEDs and MED.

b) High voltage distribution and test pulse generator input sections for HEDs.

Figure 6 Gas control system.

Figure 7 Pulse height distribution for X-rays entering LED 1 from a bright region in Hercules(□), a typical sky region (o), the dark Earth (Δ), and with the protective covers closed (x). Error bars shown are 1σ statistical uncertainties only.

Figure 8 Counting rates for 3° x 3° and 1 1/2° x 3° fields of view LED 1 while viewing the Earth as a function of the anti-coincidence rate.

Figure 9 Counting rate for 3° x 3° and 1 1/2° x 3° fields of view on LED 1 in the 0.15 - 0.30 keV range while viewing the dark Earth as a function of charged particle counting rate (Ne).

Figure 10 Counting rate of charged particles versus angle between the magnetic field vector and the detector viewing axis. for LED 1. This includes data taken approaching the normal to the magnetic field (x) and receding from the normal (·).

Figure 11 X-ray counting rate (1/4 keV channel) LED 1 versus angle of detector viewing axis to the center of the Earth. The 3° x 3° section is represented by the solid lines, while the 1 1/2° x 3° section is denoted by the dotted lines. Data was taken while pointing at SS Cygni as the Earth slowly occulted the source.

Figure 12 Histograms of observed counting rate samples sorted according to X-ray counting rate for HED 1 for the large and small fields of view.

Figure 13 Superposed count rate versus scan angle for August 21, 1977 binned into 1/2 degree bins. The scan angle approximates ecliptic latitude with the origin at the northward crossing of the ecliptic plane. All data are from the 3° x 3° field of view collimator sections. The energy ranges and detectors are noted beside each trace.

Figure 14 Superposed count rate versus scan angle on the sky for the 3° x 3° field of view on HED 1. The peak at a scan angle of $\sim$ 73° is attributed to AM HER. DQ HER is excluded. An Abell cluster (A2256) was at the edge of the scan path.

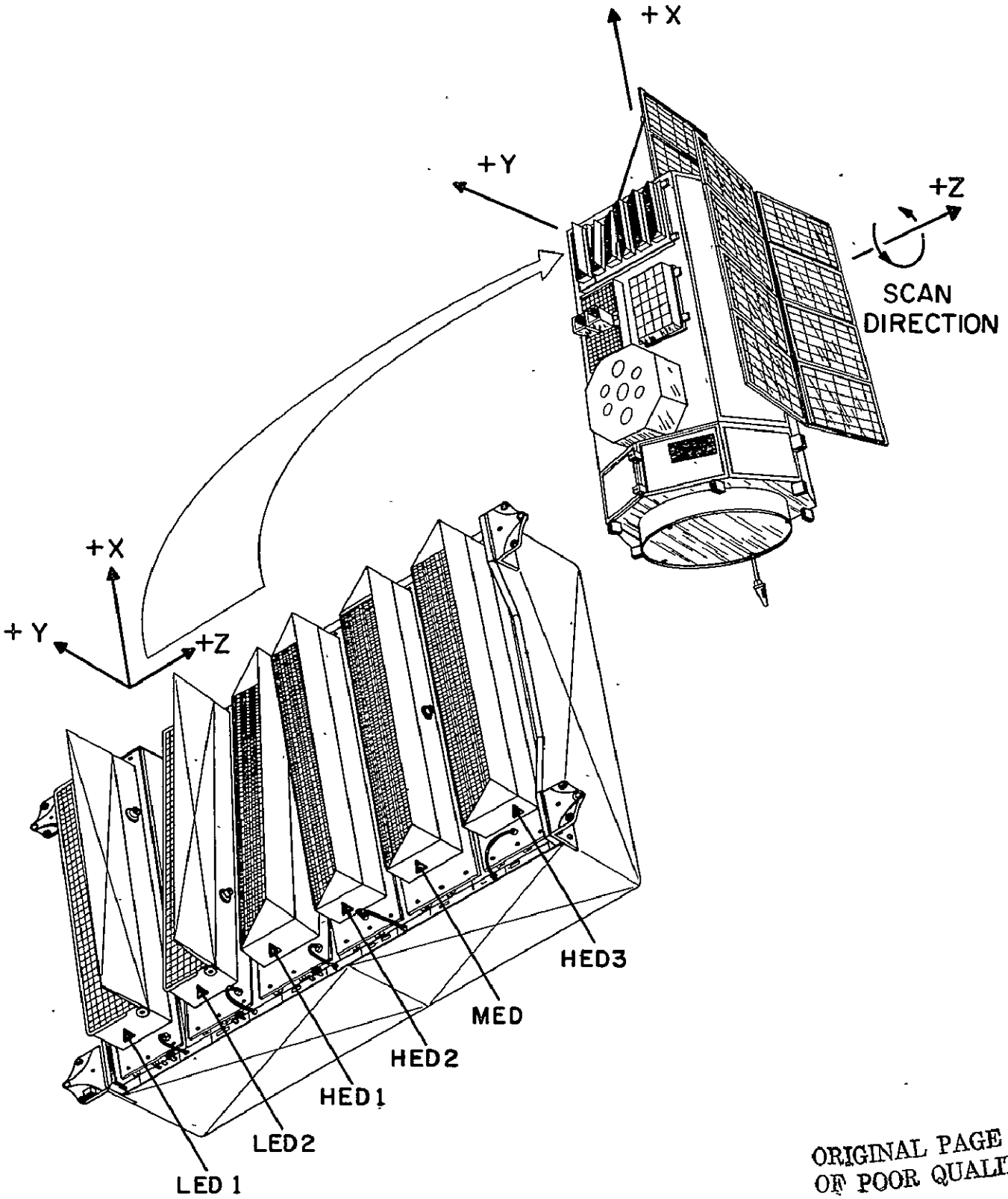

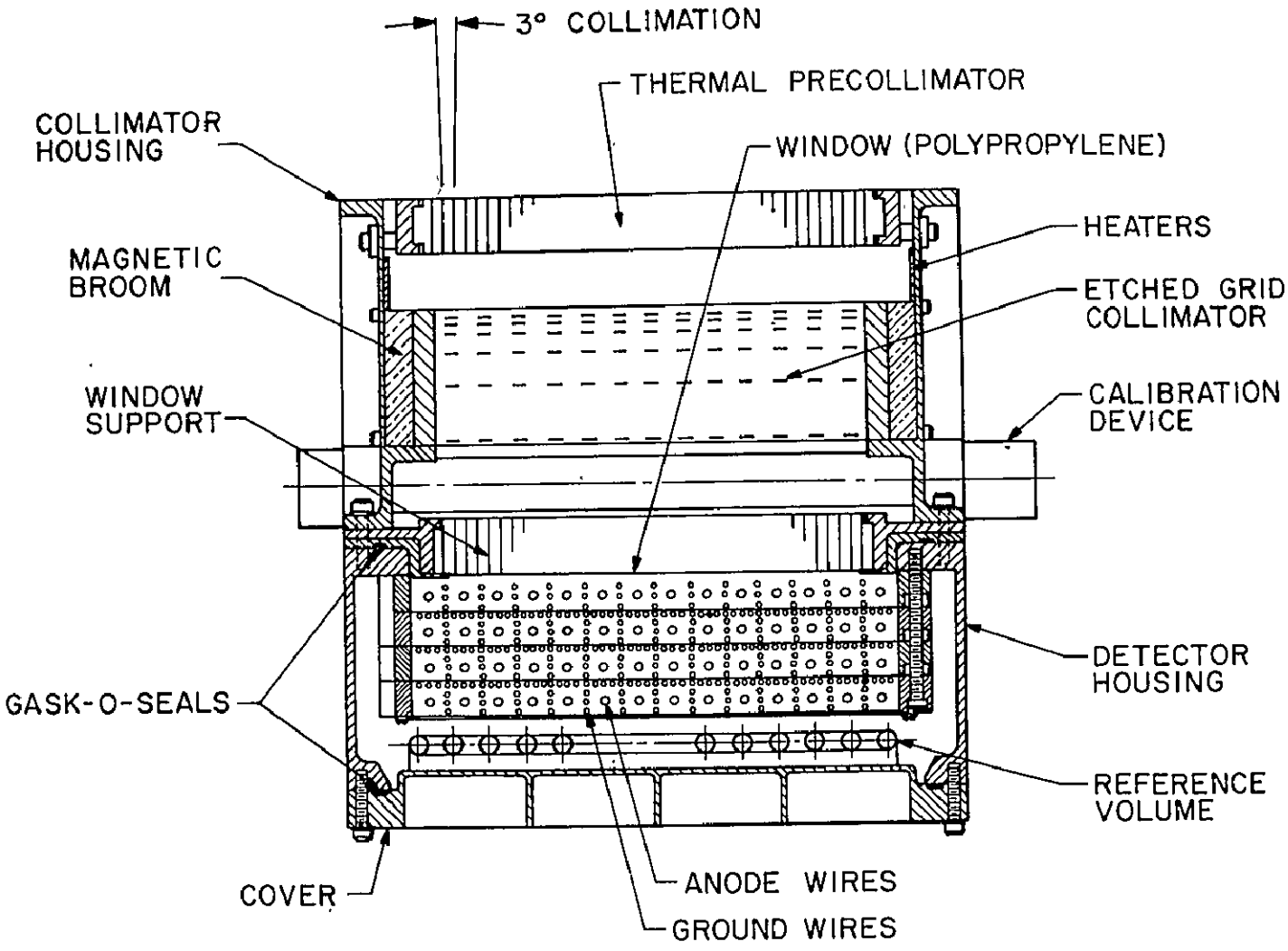

LED CROSSECTION

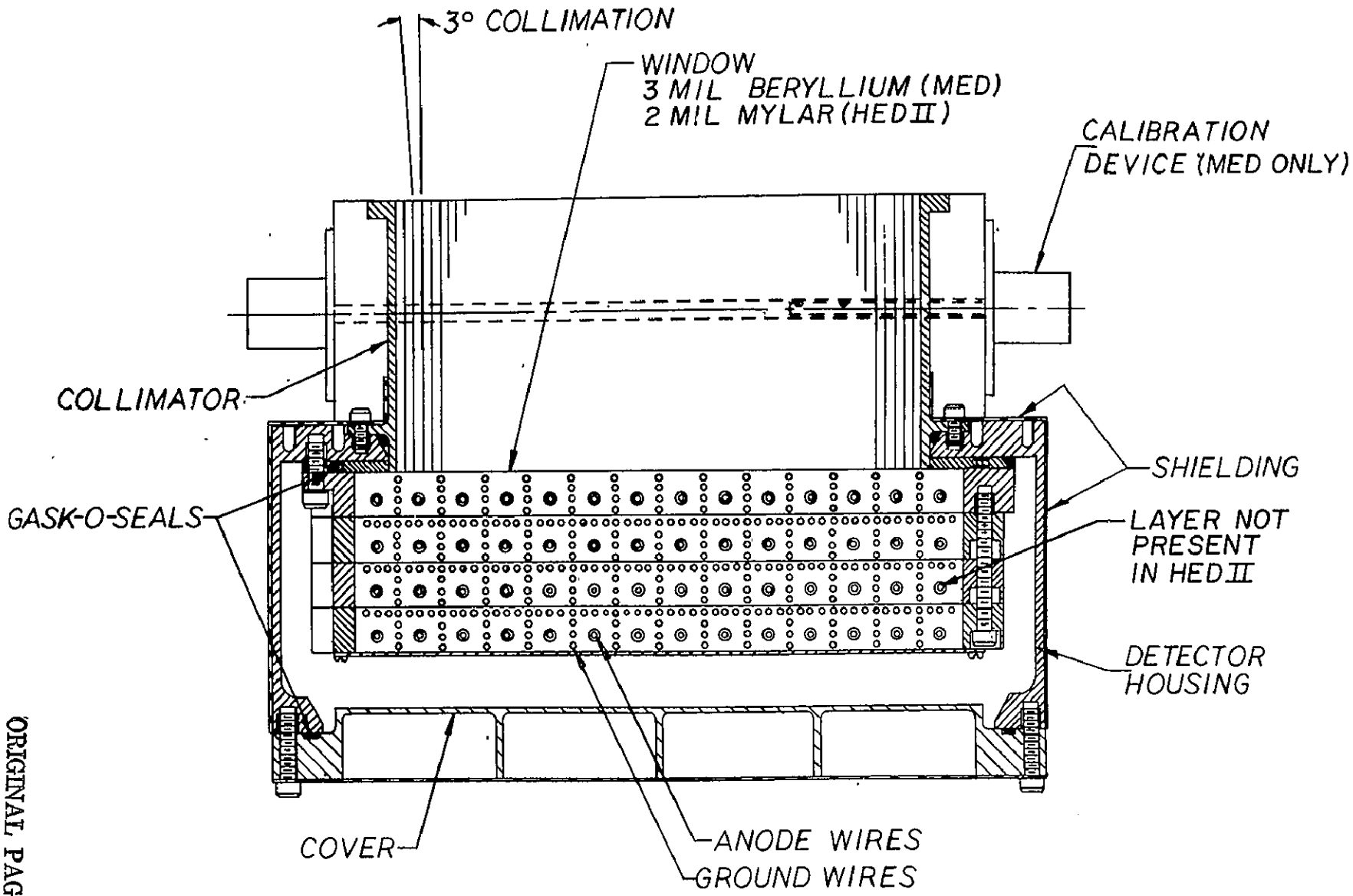

MED / HED II CROSSECTION

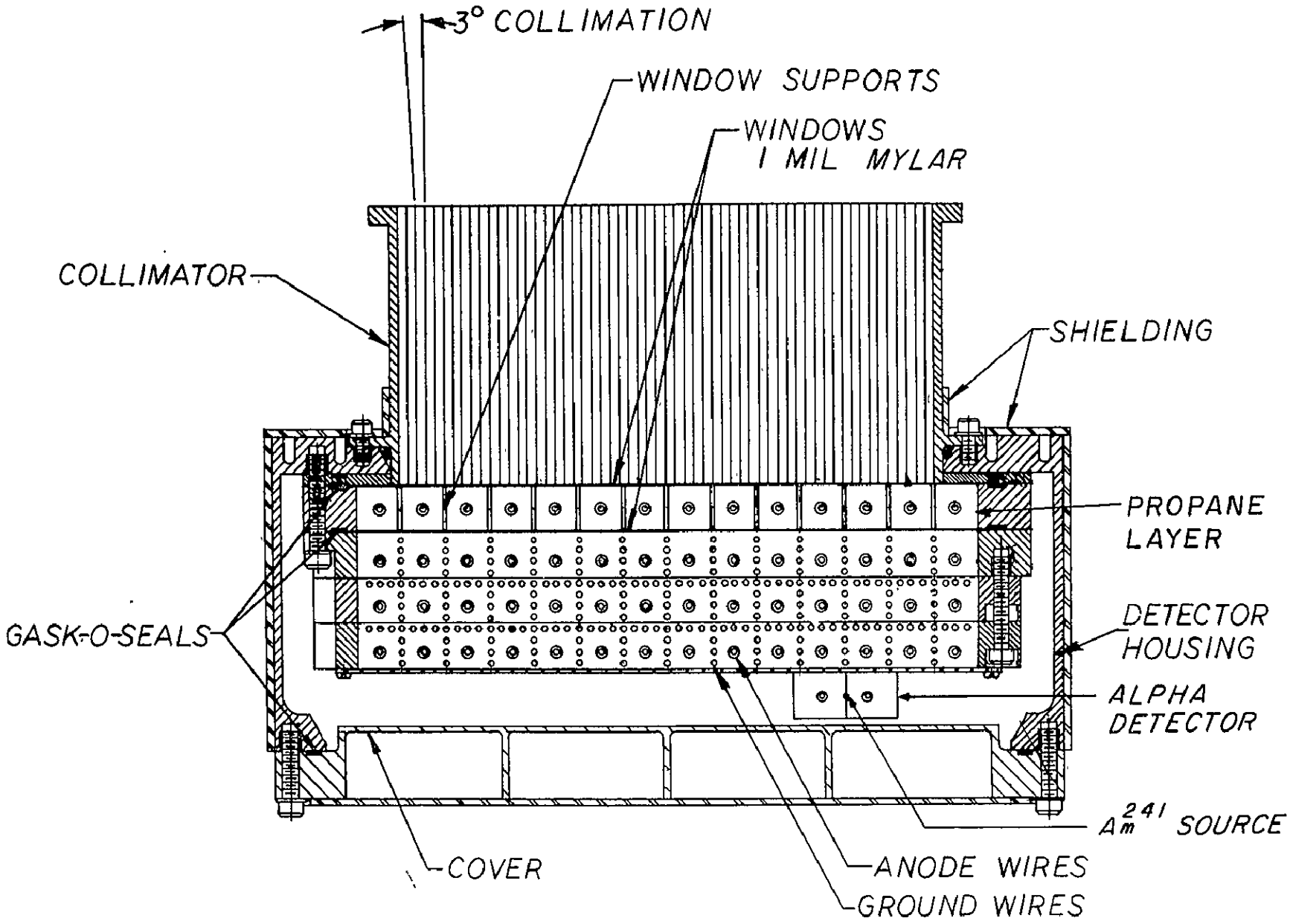

HED CROSS SECTION

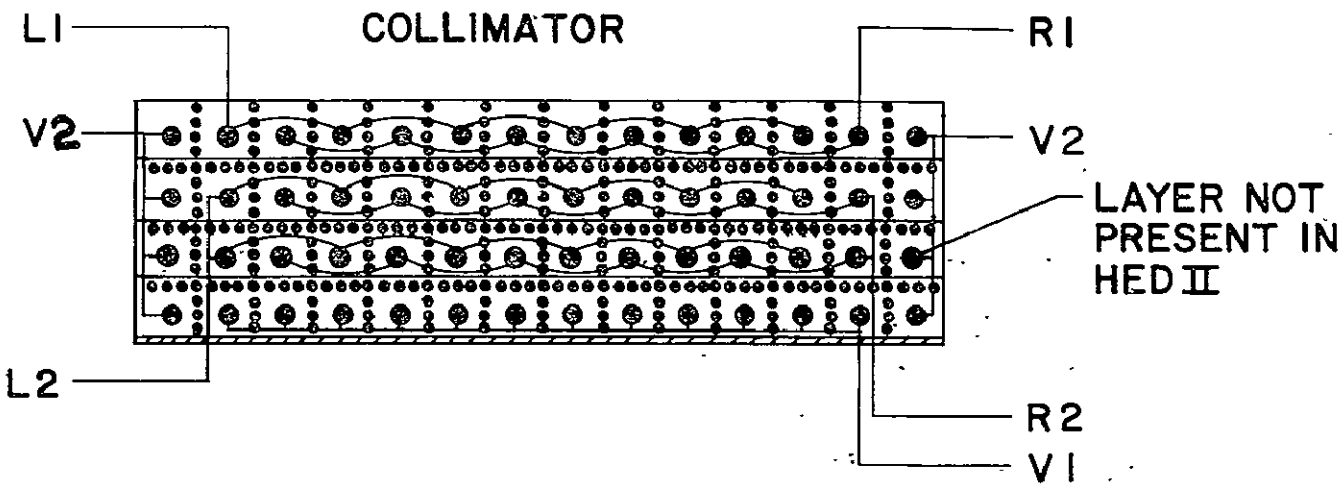

LED, MED, HED II

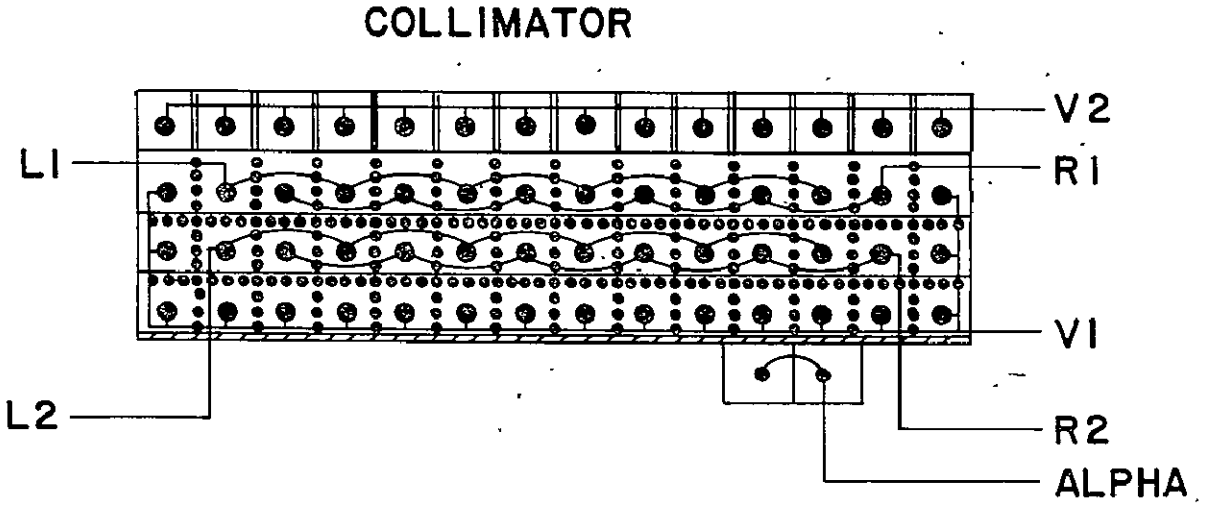

HED I/III

DETECTOR GRID CONNECTIONS

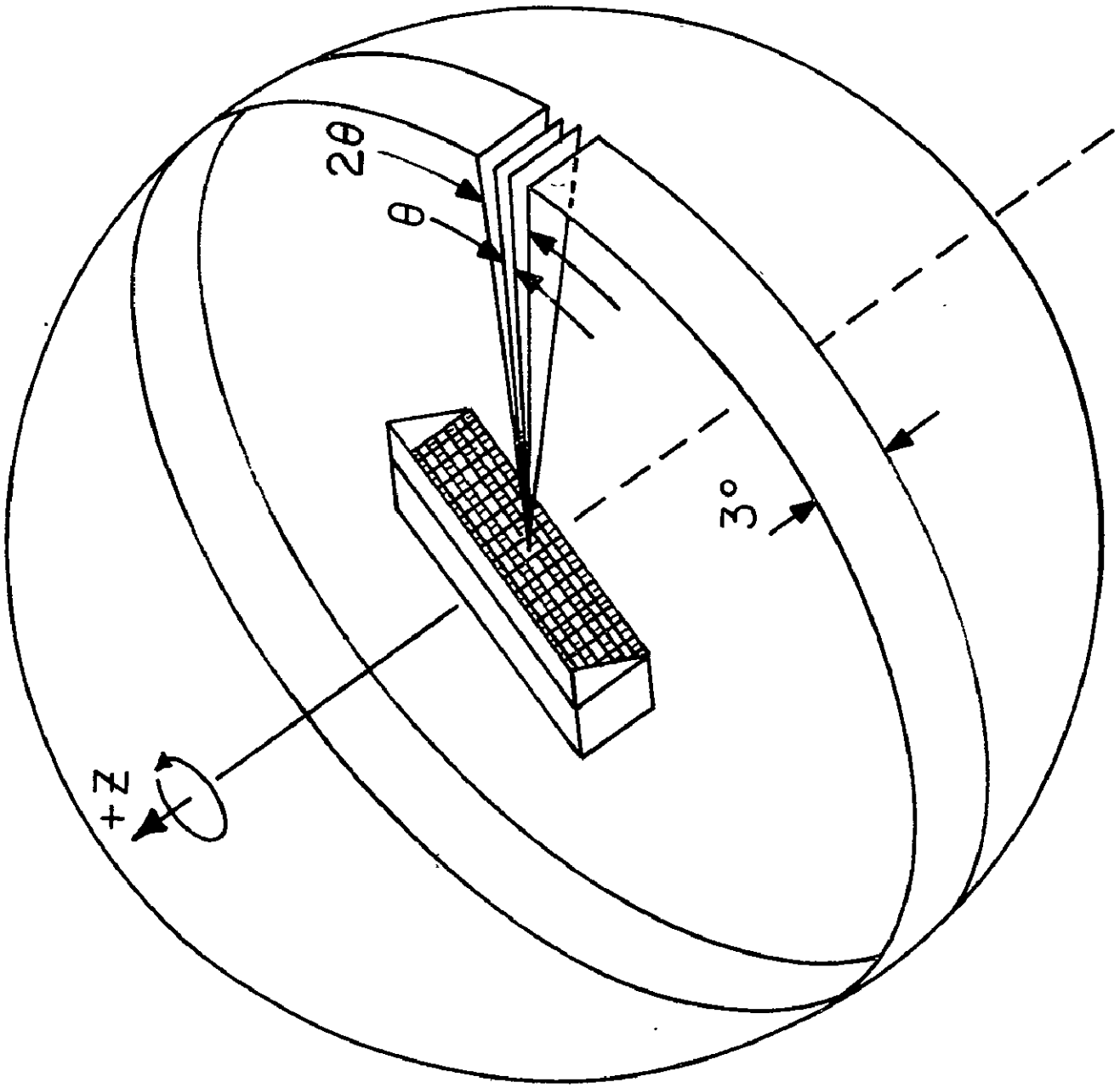

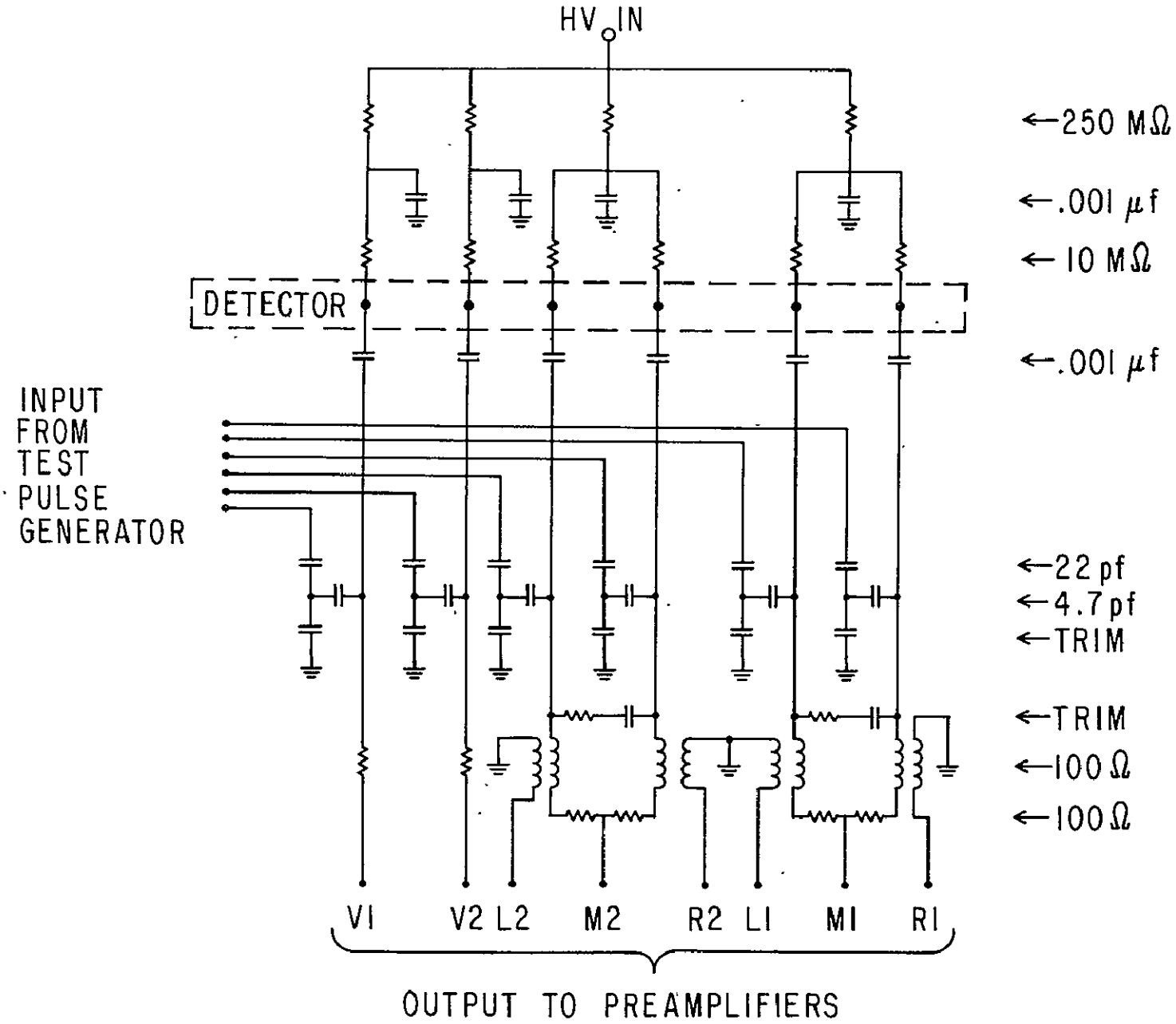

LOW AND MEDIUM ENERGY DETECTOR FRONT END SECTION

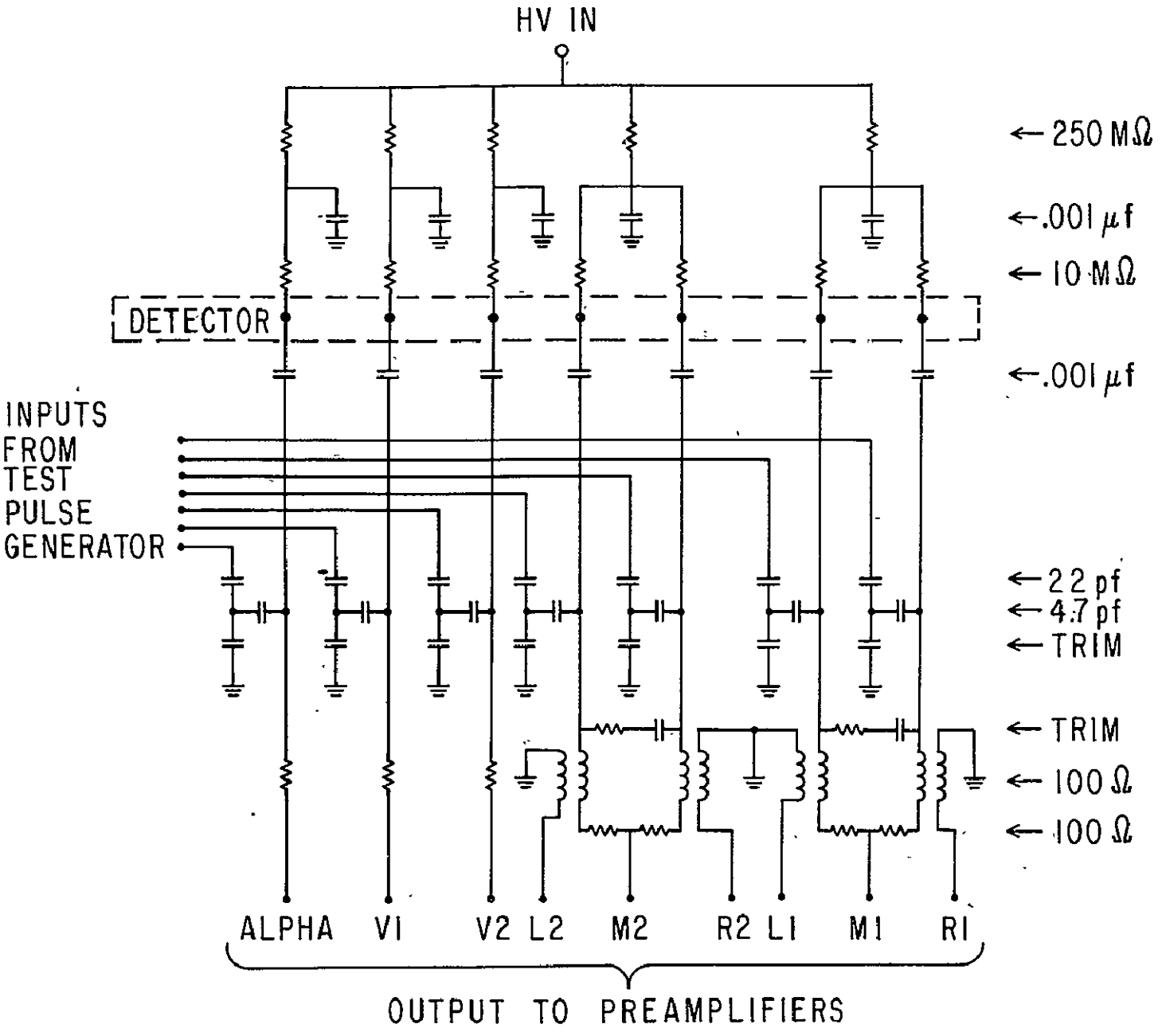

HIGH ENERGY DETECTOR FRONT END SECTION

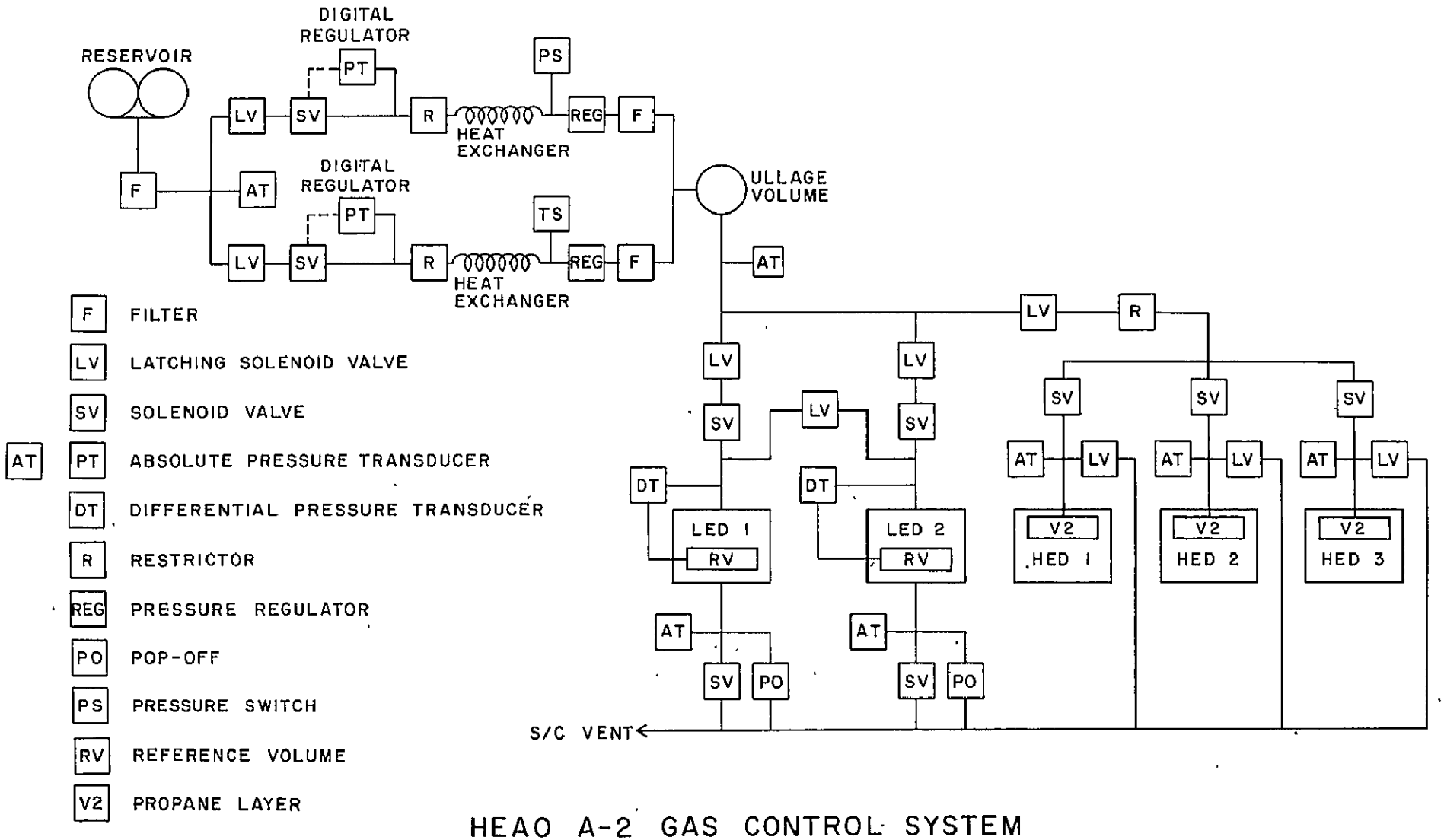

HEAO A-2 GAS CONTROL SYSTEM

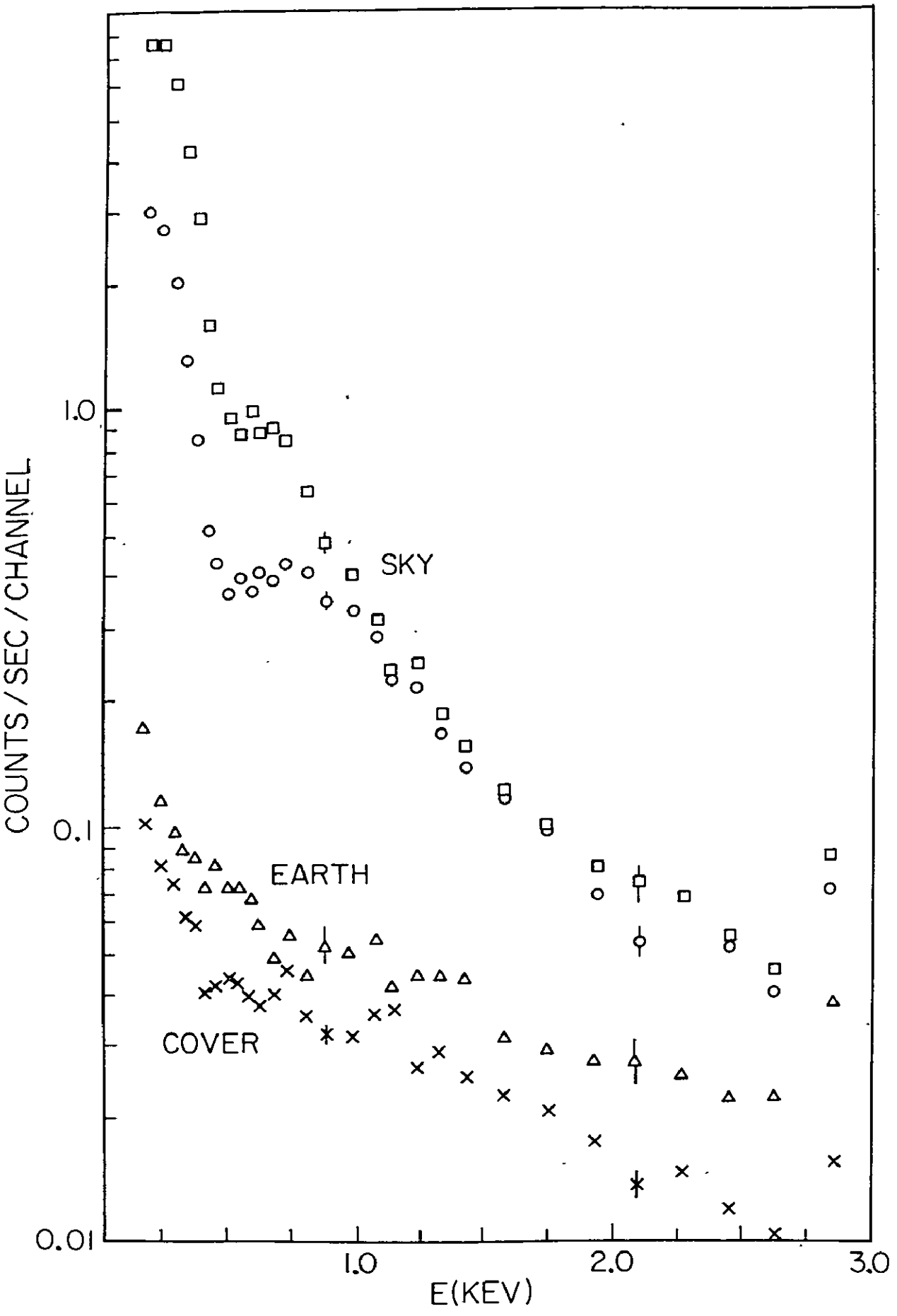
COUNTS / SEC / CHANNEL
1.0
0.1
0.01
SKY
EARTH
COVER
1.0
2.0
3.0
E(KEV)

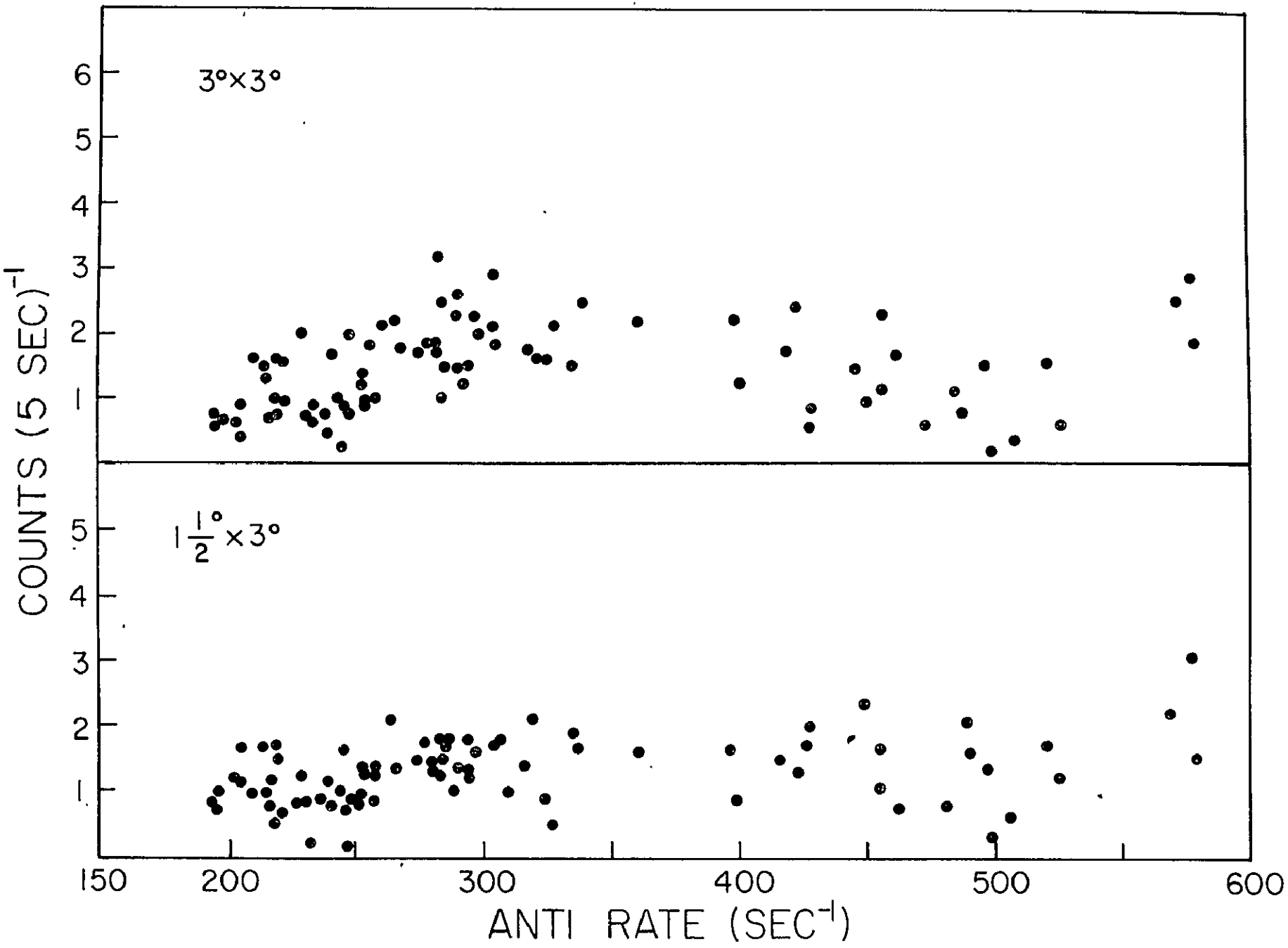
3°×3°
1½°×3°
COUNTS (5 SEC)⁻¹
ANTI RATE (SEC⁻¹)
150
200
300
400
500
600

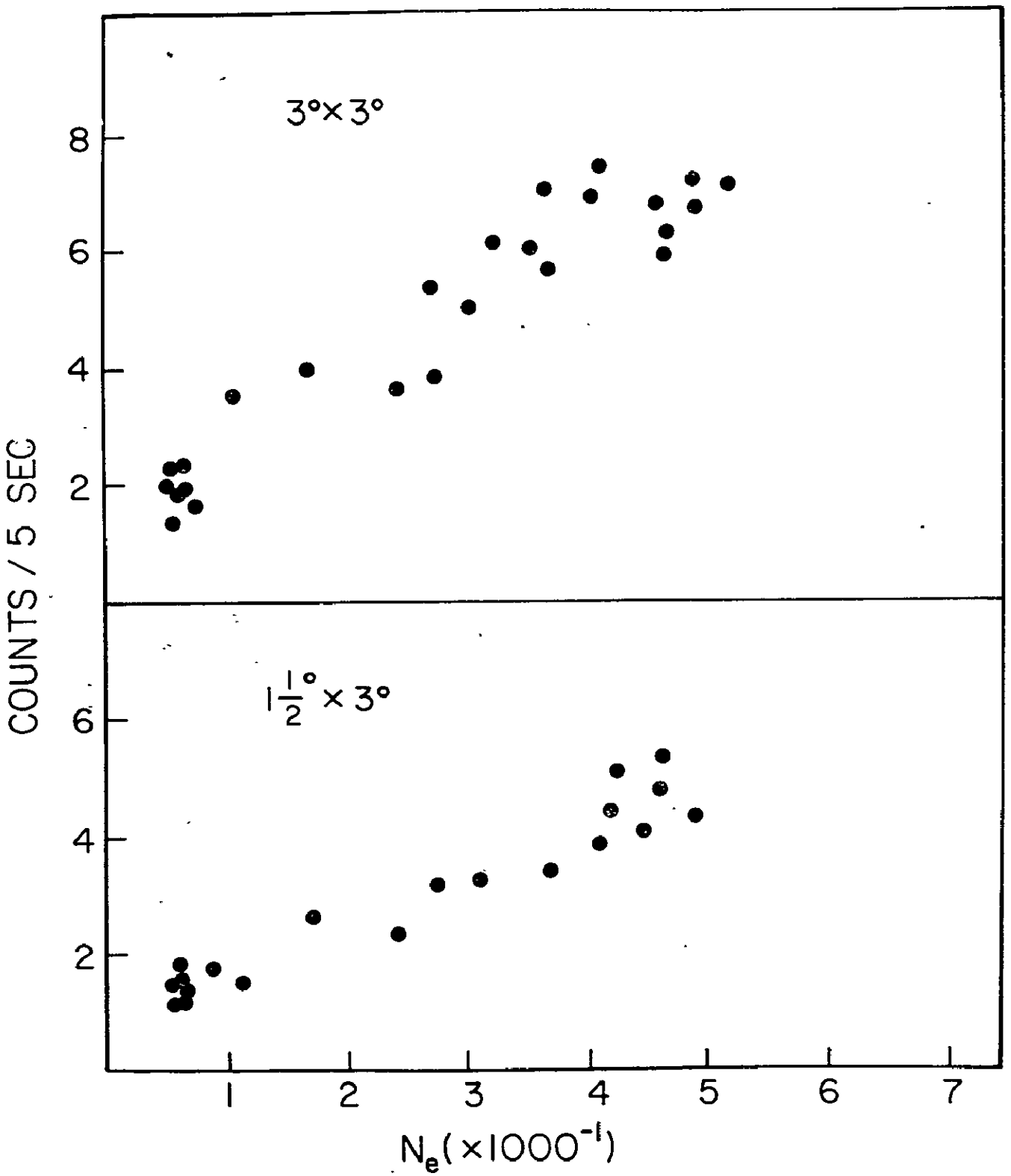
3°×3°
1½°×3°
COUNTS / 5 SEC
2
4
6
8
2
4
6
1
2
3
4
5
6
7
$N_e(\times 1000^{-1})$

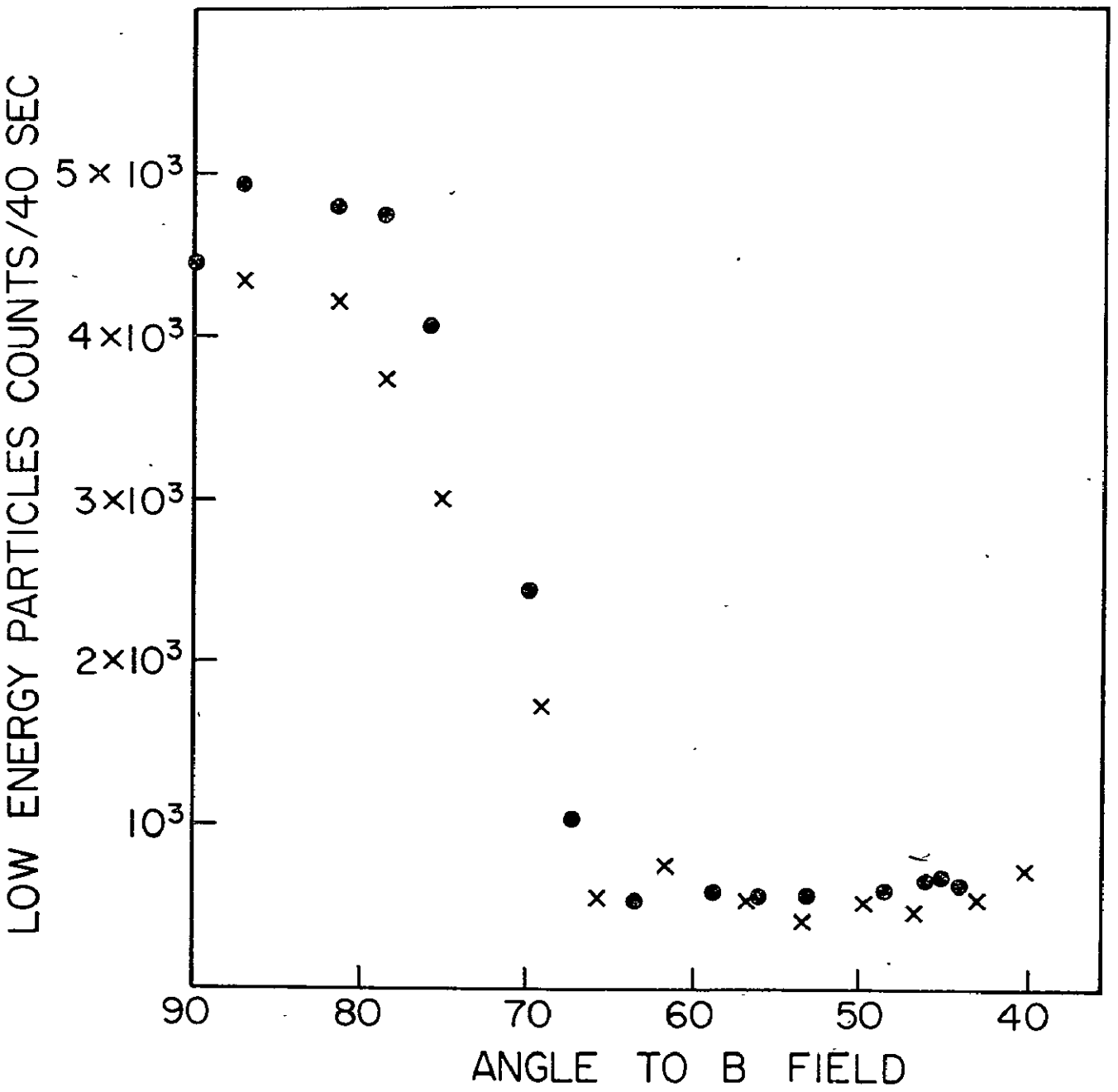
LOW ENERGY PARTICLES COUNTS/40 SEC
5 x 10³
4x10³
3x10³
2x10³
10³
90
80
70
60
50
40
ANGLE TO B FIELD

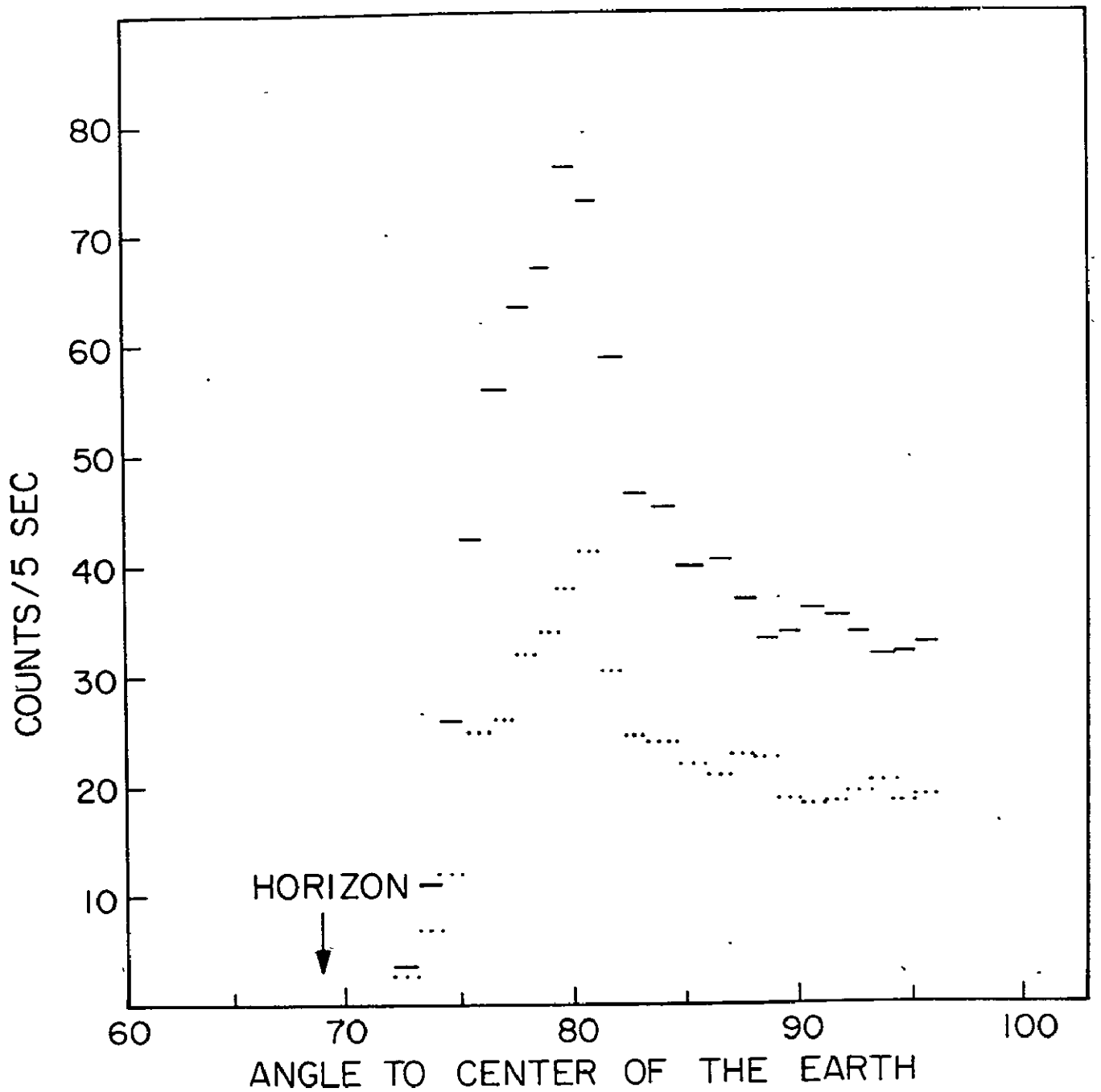

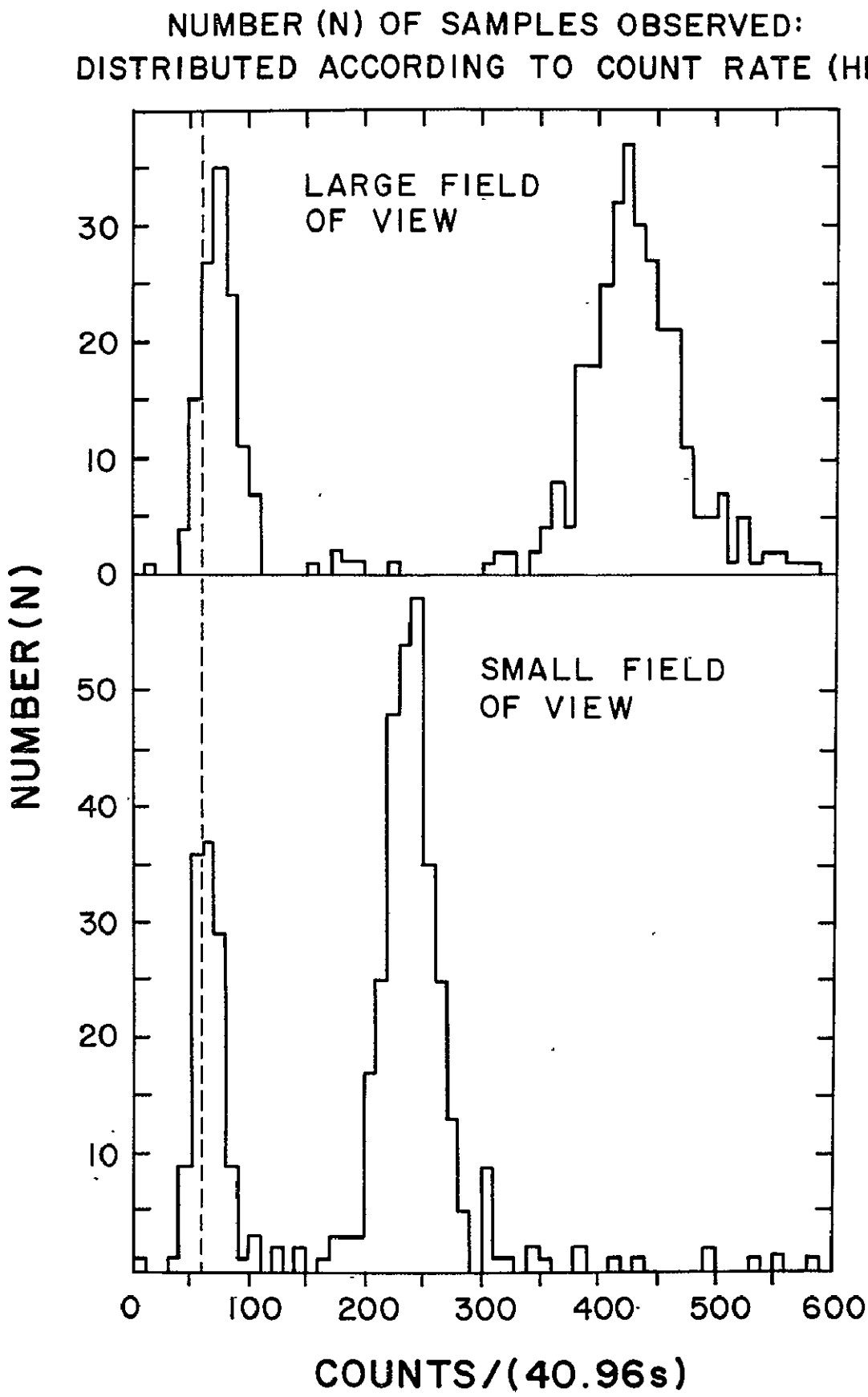
NUMBER (N) OF SAMPLES OBSERVED:
DISTRIBUTED ACCORDING TO COUNT RATE (HEDI)
LARGE FIELD
OF VIEW
SMALL FIELD
OF VIEW
NUMBER (N)
0
10
20
30
40
50
0
100
200
300
400
500
600
COUNTS/(40.96s)

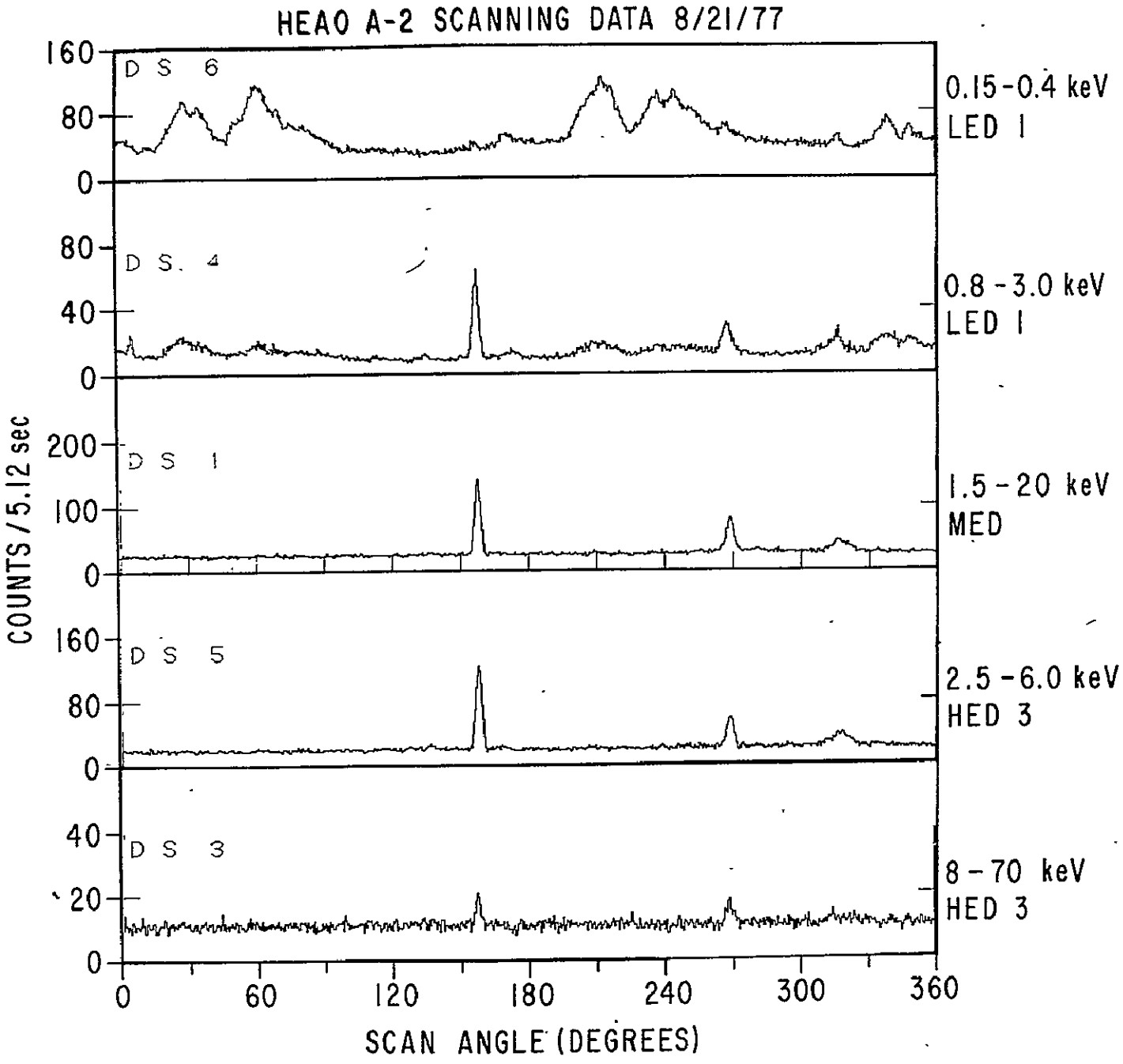

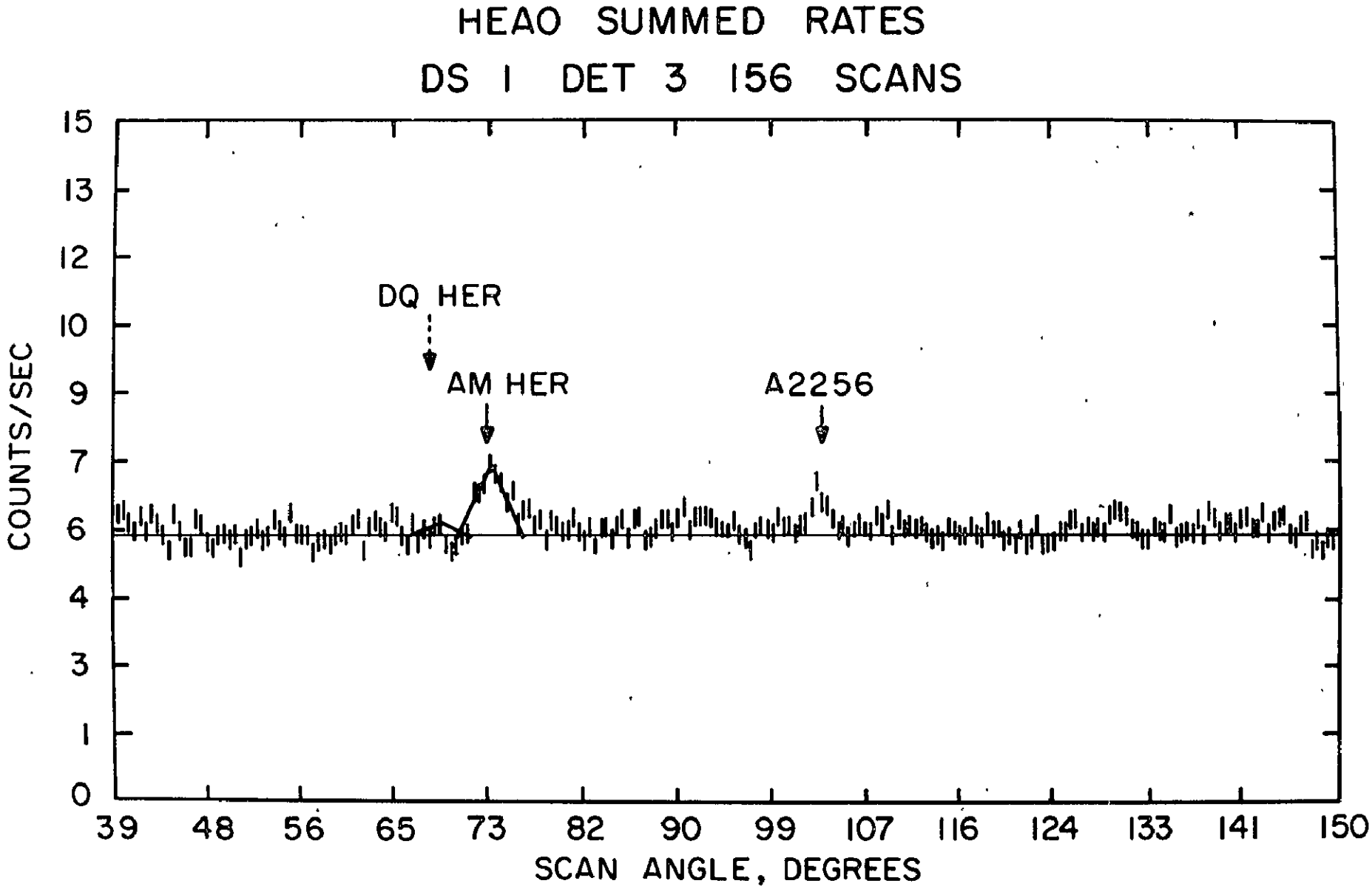
HEAO SUMMED RATES
DS 1 DET 3 156 SCANS
DQ HER
AM HER
A2256
COUNTS/SEC
0
1
3
4
6
7
9
10
12
13
15
39
48
56
65
73
82
90
99
107
116
124
133
141
150
SCAN ANGLE, DEGREES

BIBLIOGRAPHIC DATA SHEET

1. Report No.	2. Government Accession No.	3. Recipient's Catalog No.
4. Title and Subtitle THE COSMIC X-RAY EXPERIMENT ABOARD HEAO-1		5. Report Date June 1978 6. Performing Organization Code 661
7. Author(s) R. Rothschild (UCSD), E. Boldt, S. Holt, P. Serlemitsos		8. Performing Organization Report No.
9. Performing Organization Name and Address Code 661 Cosmic Radiations Branch Laboratory for High Energy Astrophysics		10. Work Unit No. 11. Contract or Grant No. 13. Type of Report and Period Covered
12. Sponsoring Agency Name and Address		14. Sponsoring Agency Code

15. Supplementary Notes

16. Abstract

The Cosmic X-ray Experiment aboard the HEAO-1 observatory is described. The instrument consists of six gas proportional counters of three types nominally covering the energy ranges of 0.15 - 3 keV, 1.2 - 20 keV, and 2.5 - 60 keV. The two low energy detectors have about 400 cm^2 open area each while the four others have about 800 cm^2 each. A novel feature of this experiment is the dual field of view collimators that allow the unambiguous determination of instrument internal background and diffuse X-ray brightness. Instrument characteristics and early performance will be discussed.

17. Key Words (Selected by Author(s))	18. Distribution Statement		
19. Security Classif. (of this report) U	20. Security Classif. (of this page) U	21. No. of Pages 62	22. Price*

*For sale by the National Technical Information Service, Springfield, Virginia 22151.